Design, synthesis of combretastatin A-4 piperazine derivatives as potential antitumor agents by inhibiting tubulin polymerization and inducing autophagy in HCT116 cells

Hangqi Zhang, Ming Li, Xueming Zhou, Li Tang, Guangying Chen, Yongmin Zhang

Design, synthesis of combretastatin A-4 piperazine derivatives as potential antitumor agents by inhibiting tubulin polymerization and inducing autophagy in HCT116 cells

10.1016/j.ejmech.2024.116497

Hangqi Zhang [a], Ming Li [a], Xueming Zhou [a], Li Tang [a], Guangying Chen [a,*], Yongmin Zhang [a,b,**]

[a] *Key Laboratory of Tropical Medicinal Resource Chemistry of Ministry of Education and Key Laboratory of Tropical Medicinal Plant Chemistry of Hainan Province, College of Chemistry and Chemical Engineering, Hainan Normal University, Haikou, Hainan 571158, China*

[b] *Sorbonne Université, CNRS, Institut Parisien de Chimie Moléculaire, UMR 8232, 4 Place Jussieu, 75005 Paris, France*

** Corresponding author. Key Laboratory of Tropical Medicinal Resource Chemistry of Ministry of Education and Key Laboratory of Tropical Medicinal Plant Chemistry of Hainan Province, College of Chemistry and Chemical Engineering, Hainan Normal University, Haikou, Hainan 571158, China*

*** Corresponding author. Sorbonne Université, CNRS, Institut Parisien de Chimie Moléculaire, UMR 8232, 4 Place Jussieu, 75005 Paris, France*

E-mail addresses: chgying123@163.com (GC), yongmin.zhang@upmc.fr (YZ).

ABSTRACT

A series of combretastatin A-4 (CA-4) derivatives were designed and synthesized, which contain stilbene core structure with different linker, predominantly piperazine derivatives. These compounds were evaluated for their cytotoxic activities against four cancer cell lines, HCT116, A549, AGS, and SK-MES-1. Among them, compound **13** displayed the best effectiveness with IC_{50} values of 0.227 μM and 0.253 μM against HCT116 and A549 cells, respectively, showing low toxicity to normal cells. Mechanistic studies showed that **13** inhibited HCT116 proliferation via arresting cell cycle at the G2/M phase through disrupting the microtubule network and inducing autophagy in HCT116 cells by regulating the expression levels of autophagy-related proteins. In addition, **13** displayed antiproliferative activities against A549 cells through blocking the cell cycle and inducing A549 cells apoptosis. Because of the poor water solubility of **13**, four carbohydrate conjugates were synthesized which exhibited better water solubility. Further investigations revealed that **13** showed positive effects *in vivo* anticancer study with HCT116 xenograft models. These data suggest that **13** could be served as a promising lead compound for further development of anti-colon carcinoma agent.

Keywords: CA-4; Piperazine derivatives; Synthesis; Carbohydrate; Antitumor; Cell cycle.

1 Introduction

Cancer is the second leading cause of death after cardiovascular disease, which is

a major problem of public health worldwide [1]. Colorectal cancer (CRC) is a widely observed tumor of the digestive tract, ranking third in frequency of diagnosis [2, 3]. It is also an extremely malignant tumor which has become the fourth leading cause of cancer-related death [3]. This type of cancer causes almost 900,000 deaths annually, accounting for 9.2% of all deaths worldwide [3, 4]. It is worth noting that according to statistics from the American Cancer Society in 2023, the number of young patients dying from CRC increased between 2005-2020 [5]. Currently, therapeutic medications which used clinically to treat CRC, including capecitabine, 5-FU and oxaliplatin are prone to causing significant toxicity and exacerbating chemotherapy resistance [6, 7]. Therefore, it is desirable to develop safe and effective drugs to treat this disease [8].

Combretastatin A-4, a *cis* stilbene derivative, which was collected from South African bush willow tree, the bark of the *Combretum caffrum* [9], could damage the cytoskeleton leading to cell death by combining with tubulin and destabilizing microtubules [10, 11].

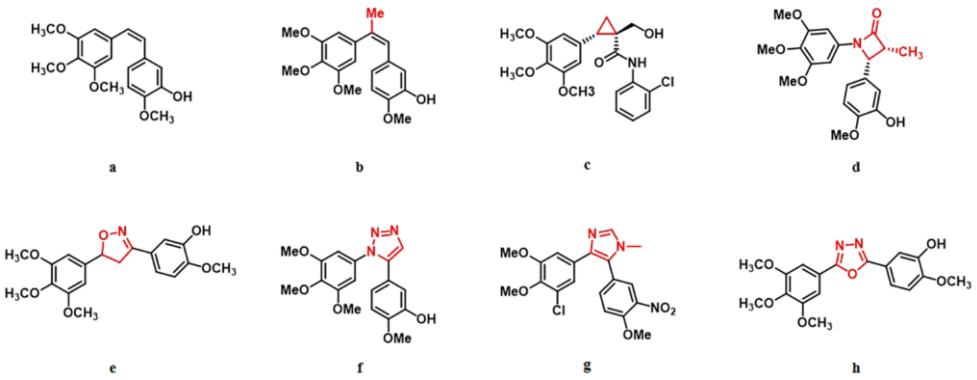

Fig. 1. CA-4 (a) and olefinic bond protection strategies of CA-4 derivatives, include addition onto ethylene bond (b); cyclopropylamide (c); β-lactam (d); isoxazoline (e); triazole (f); imidazole (g) and

oxadiazole (h).

CA-4 is composed of three important pharmacophores, the olefinic bond with *cis* configuration as linker and two substituted hydrophobic benzene rings. Importantly, the olefin bridge with (Z)-configuration plays a vital role in biological activity, which is essential for binding at appropriate distance at the colchicine site [12, 13]. According to the previous reports, CA-4 displayed excellent effectiveness against a variety of malignant cancers, such as breast cancer, lung cancer, cervix cancer and colon cancer [14]. However, the unstable olefinic bond which is prone to isomerization, from *cis* to less antitumor activity *trans*, and poor water solubility have greatly limited the development of its clinical application [15, 16].

In recent years, some excellent CA-4 analogues have been synthesized in different strategies by many research groups, for instance, addition of substituents onto the olefinic bond [17, 18], replacing ethylene bond with a rigid heterocyclic ring, included tricyclic heterocycles (cyclopropylamide analogues) [19], tetracyclic heterocycles (chiral β-lactam bridged analogues) [20], pentacyclic heterocycles (isoxazoline [21], triazole [22-25], imidazole [26] and oxadiazole [27] analogues) (Fig. 1). Piperazine and its substituted heteroaryl piperazinyl carbonyl derivatives possess potent anticancer activity [28-30]. Additionally, arylpiperazine structure has been considered as a privileged scaffold [31], and a series of compounds containing this type of scaffold have been reported as tubulin polymerization inhibitors [32, 33] (Fig. 2). Inspired by this, we introduced phenylpiperazine containing different types and different position substituents on CA-4 to obtain a series of structural

modifications derivatives.

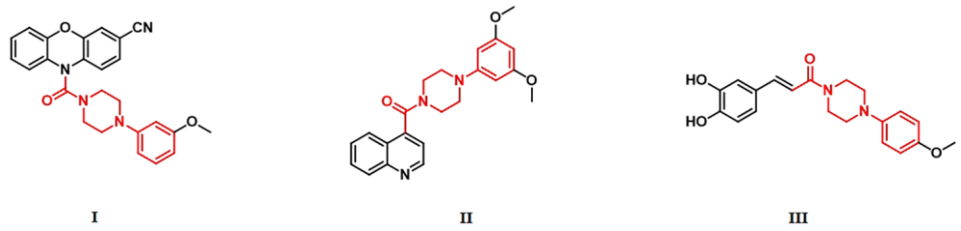

Fig. 2. Phenylpiperazine scaffold inhibitors of tubulin polymerization.

We introduced carboxyl functional groups on the double bonds of CA-4 via perkin reaction. After investigating the antitumor activities of different nitrogen heterocycle linking arms, a series of compounds with piperazine phenyl groups and piperazine benzyl groups were synthesized. Some derivatives were evaluated for their cytotoxic activities against four cancer cell lines, including human colon cancer cells HCT116, non-small cell lung cancer cells A549, human gastric adenocarcinoma cells AGS and human lung squamous cell carcinoma SK-MES-1. These derivatives exhibited cytotoxic activities against cancer cell lines with IC_{50} values from 0.227 μM to 3.636 μM. Among these compounds, **13** displayed the best effectiveness which could significantly inhibit the proliferation of colon cancer and lung cancer. In order to elaborate on the basis of the antitumor activity of **13**, we also performed some mechanism studies. Moreover, **13** was evaluated for *in vivo* antitumor activity against colon cancer in a mouse xenograft model. The results suggest that **13** could deserves further preclinical evaluation as a potential lead compound for the treatment of colon cancer.

2 Results and discussion

2.1. Chemistry

Here, acrylic acid **A** was synthesized by using the perkin reaction, which 3,4,5-Trimethoxyphenylacetic acid with 3-Hydroxy-4-methoxybenzaldehyde was refluxed in the presence of triethylamine and acetic anhydride [34] (Scheme 1). And then, compound **A** was coupled with pyrrolidine, morpholine, piperazine, thiomorpholine and thiomorpholine-1,1-dioxide respectively in dichloromethane (DCM), 1-Ethyl-3-(3-dimethylaminopropyl) carbodiimide (EDCI) was used to form amide bond and Hydroxybenzotriazole (HOBT) has been added as a catalyst. In addition, N, N-Diisopropylethylamine (DIPEA) played as an acid binding in the reaction [35] (Scheme 2). Under the same conditions, the synthesis of piperazine amide derivatives **6**-**22** was initiated from acrylic acid **A**, the substituted piperazines included fluorophenyl, chlorophenyl, bromophenyl, methylphenyl, methoxyphenyl and some other types of substituted groups (Scheme 3).

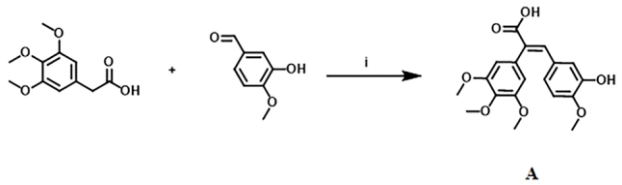

Scheme 1. Synthesis of compound **A**. Reagents and conditions: (i) Et_3N, Acetic anhydride, reflux, 6 h, 41%.

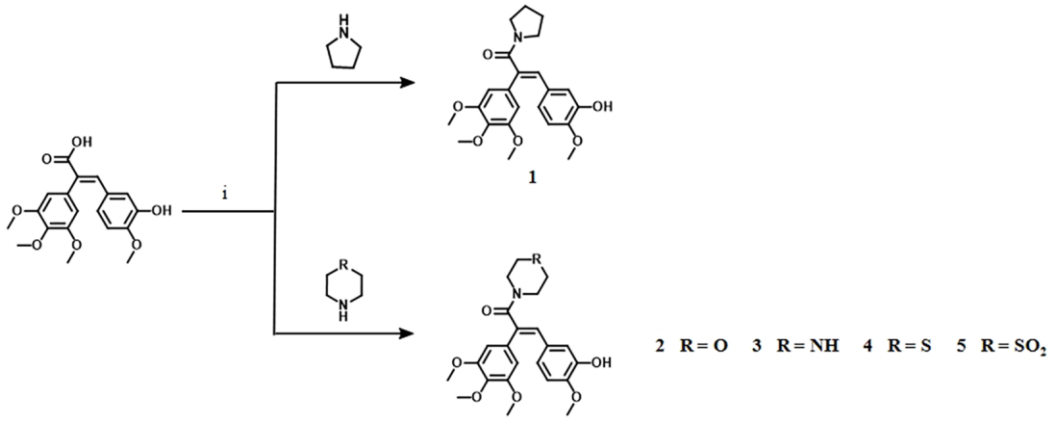

Scheme 2. Synthesis of Combretastatin A-4 heterocycle derivatives. Reagents and conditions: (i) EDCI, HOBT, DIPEA, DCM, rt, 12 h, 35%-46%.

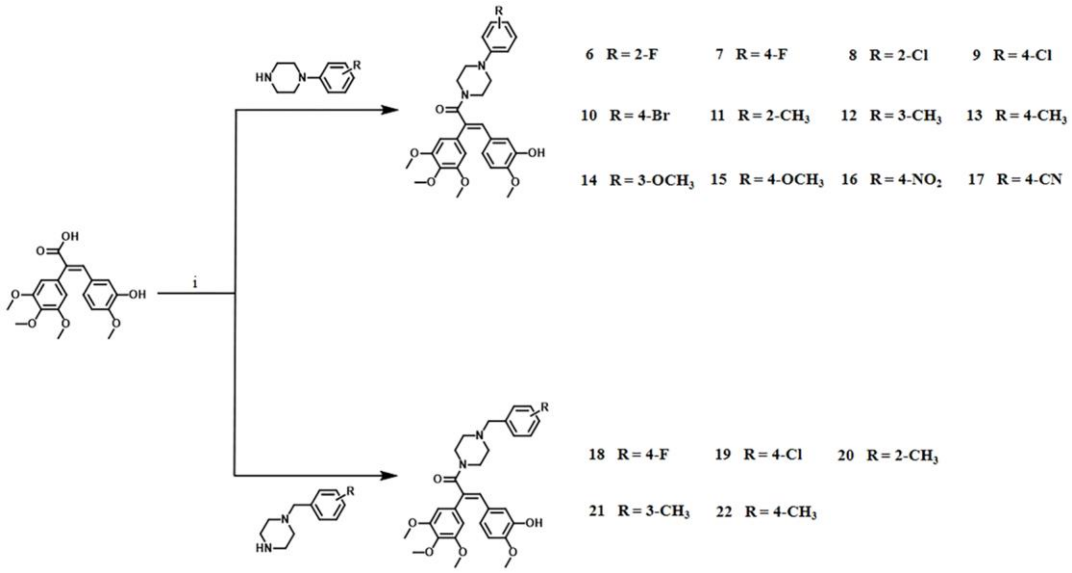

Scheme 3. Synthesis of Combretastatin A-4 piperazine derivatives. Reagents and conditions: (i) EDCI, HOBT, DIPEA, DCM, rt, 12 h, 40%-47%.

Glucose, galactose, mannose and lactose were used for the synthesis of **36-39**. They were treated with acetic anhydride and sodium acetate in reflux in order to obtain **23-26** which with all hydroxyl groups protected by acetyl groups. And then, **23-25** were suffered Hydrobromic acid (33% HBr in Acetic acid) to selectively transform anomeric acetyl group to bromine, which the donors **27-29**. Next, glycosylation of compound **13** with the donors were performed in DCM in the presence of NaOH and tetra-

butylammonium fluoride (TBAF) to give intermediate **32**-**34**. Subsequently, the intermediates deacetylated in methanol with K_2CO_3, target molecule **36**-**38** were carried out in good yield. Due to the special conformation of mannose, Schmidt Glycosylation was used to obtain the mannose conjugate of compound **13**. Benzylamine was added in the tetrahydrofuran (THF) with **26** overnight in order to remove the acetyl group from the hydroxyl group at position 1. After getting the intermediate **30**, trichloroacetonitrile was used to synthesize donor **31** under an inert atmosphere at 0℃ with 1,8-Diazabicyclo [5.4.0] undec-7-ene (DBU). Glycosylation of compound **13** with the donor **31** were performed in dry DCM with 4 Å molecular sieves and boron trifluoride diethyl etherate at -40℃ to obtain the target intermediate **35**. Next, intermediate **35** deacetylated under the same conditions like **32**-**34** and we got the target compound **39** (Scheme 4). For the characterization of NMR (^{1}H) spectra, NMR (^{13}C) spectra and HRMS of compounds, please refer to the supplementary information. The results of oil-water partition coefficient indicated that the sugar conjugates of compound **13** were more hydrophilic than their original compound (Table 1).

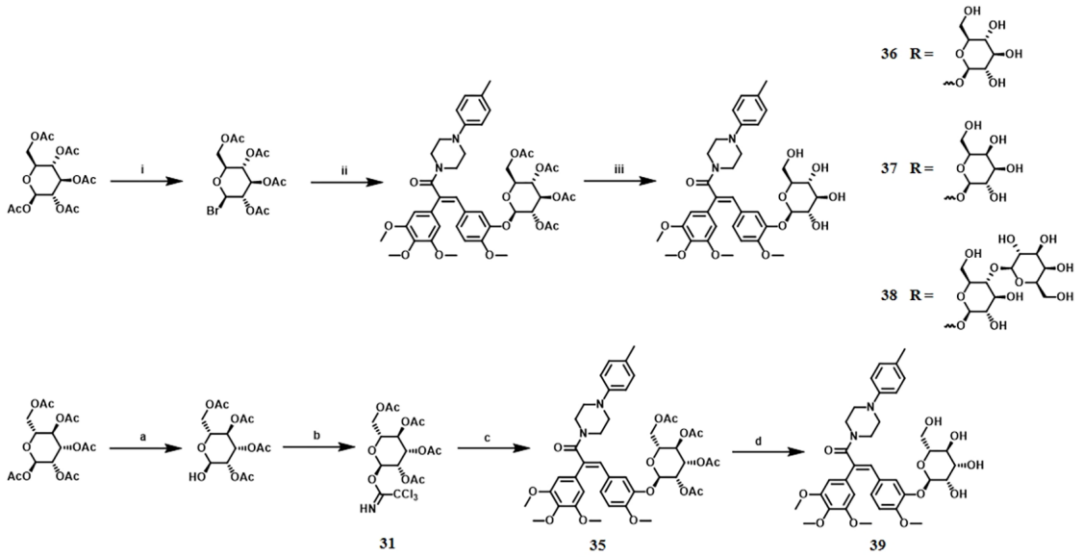

Scheme 4. Synthesis of compound **13** sugar conjugates. Reagents and conditions: (i) HBr (33 wt.% in Acetic acid); (ii) compound **13**, TBAF, K_2CO_3, 59-68%; (iii) MeOH, K_2CO_3, 98%-99%; (a) THF, $BnNH_2$; (b) DCM, DBU, CCl_3CN, 77%; (c) DCM, 4 Å molecular sieves, BF_3-Et_2O, compound **13**, 73%; (d) MeOH, K_2CO_3, 97%.

Table 1

The oil-water partition coefficient values (log *P*) of compound **36-39**, **13** and CA-4

Compound	log *P* (pH 7.4)
13	-0.013 ± 0.03
36	-0.538 ± 0.06
37	-0.432 ± 0.04
38	-0.824 ± 0.03
39	-0.638 ± 0.07
CA-4	2.143 ± 0.04

Note : Data are presented as mean ± SD (standard deviation). All experiments were independently performed at least three times.

Table 2

The cytotoxicity data of CA-4 heterocycle derivatives in HCT116 cancer cell lines

Compound	IC_{50} (μM)
1	2.482 ± 0.23
2	0.926 ± 0.12
3	**0.735 ± 0.14**
4	1.152 ± 0.07
5	1.993 ± 0.14
CA-4	0.007 ± 0.01

Note : Data are presented as mean ± SD (standard deviation). All experiments were independently performed at least three times.

Table 3

The cytotoxicity data of CA-4 piperazine derivatives in HCT116 cancer cell lines

Compound	IC_{50} (μM)
6	1.381 ± 0.13
7	0.253 ± 0.15
8	1.835 ± 0.09
9	0.593 ± 0.24
10	0.716 ± 0.13
11	1.578 ± 0.09
12	1.772 ± 0.22
13	**0.227 ± 0.12**
14	1.861 ± 0.21
15	0.941 ± 0.15
16	2.769 ± 0.23

17	3.351 ± 0.36
18	2.105 ± 0.15
19	2.691 ± 0.11
20	2.853 ± 0.12
21	3.636 ± 0.32
22	1.975 ± 0.22
CA-4	0.007 ± 0.01

Note : Data are presented as mean± SD (standard deviation). All experiments were independently performed at least three times.

2.2. Cytotoxic activities and structure-activity relationships (SAR) study

The results of cytotoxic activity were shown in (Table 2), compound **3** displayed moderate activity against HCT116 cancer cells. According to the results, **6-22** were evaluated for their cytotoxic activity against HCT116 cancer cells. As shown in (Table 3), compounds **7**, **9**, **10**, **13** and **15** displayed significant antiproliferative activities. Therefore, five compounds were evaluated for their cytotoxic activity against another three cancer cell lines (A549, AGS and SK-MES-1) with CA-4 as positive control (Table 4). The results indicated that **13** was the most effective compound against all four cancer cell lines in these compounds, with the IC_{50} values ranging from 0.227 to 0.574 μM. Compounds **7**, **9**, **10**, **13** and **15** exhibited good inhibitory activity against HCT116 but **6**, **8**, **11**, **12** and **14** showed moderate activity (IC_{50} > 1 μM) which suggested that the 4 position substituted phenylpiperazine derivatives is better than 2 or 3 position substituted. Furthermore, the inhibitory activity of **7**, **9** and **10** displayed from high to low probably due to the changed radius of the halogen substituents. In addition, electron contributing group exhibited better antitumor activity than electron withdrawing group at 4 position substituted by comparing with **13**, **16** and **17**. Importantly, the inhibitory activity of compounds which benzyl piperazine substituted is weaker than compounds which phenyl piperazine substituted, no matter where the

substituent is located on the benzene ring. A summary of the structure-activity relationships was shown in (Fig. 3). Compound **13** was further tested against normal human colon mucosal epithelial cells-NCM460 cells (Table 5).

Table 4

The cytotoxicity data of CA-4 piperazine derivatives in four cancer cell lines

Compounds	IC_{50} (μM)			
	HCT116	A549	AGS	SK-MES-1
7	0.253 ± 0.15	0.270 ± 0.13	0.531 ± 0.12	0.385 ± 0.07
9	0.593 ± 0.24	0.366 ± 0.12	1.110 ± 0.19	0.753 ± 0.06
10	0.716 ± 0.13	0.547 ± 0.27	1.348 ± 0.24	0.803 ± 0.11
13	0.227 ± 0.12	0.253 ± 0.11	0.574 ± 0.15	0.423 ± 0.14
15	0.941 ± 0.15	0.657 ± 0.22	0.882 ± 0.11	0.605 ± 0.15
CA-4	0.007 ± 0.01	0.010 ± 0.01	0.074 ± 0.01	0.007 ± 0.01

Note : Data are presented as mean ± SD (standard deviation). All experiments were independently performed at least three times.

Table 5

The cytotoxicity data of compound **13** in normal cell lines and cancer cell lines.

Compound	IC_{50} (μM)		SI
	HCT116	NCM460	
13	0.227 ± 0.12	1.090 ± 0.23	4.8
CA-4	0.007 ± 0.01	0.011 ± 0.01	1.6

SI: The index of selectivity (IC_{50} on NCM460 cells/IC_{50} on HCT116 cells).

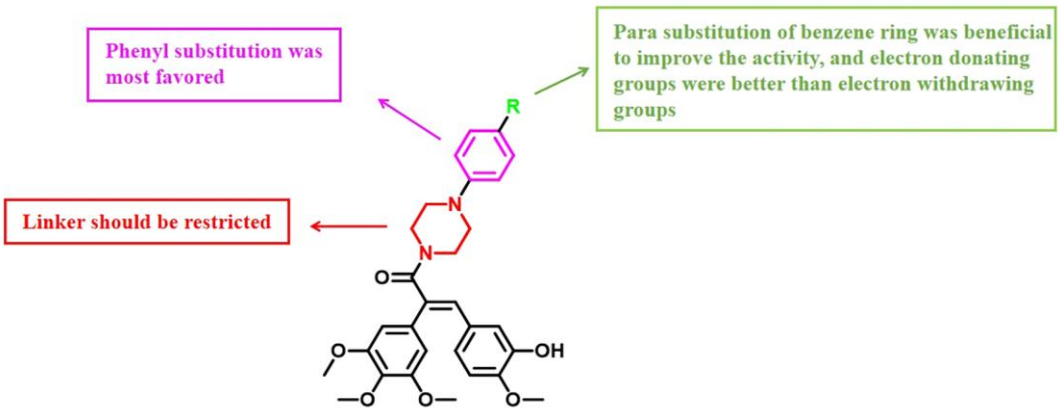

Fig. 3. Structure-activity relationships of Combretastatin A-4 piperazine derivatives as anticancer agents.

2.3. Invasion and migration

Transwell assay was used to evaluate the effects on cells invasion and migration [36, 37]. Compound **13** was chosen to test its inhibitory effects on migration and invasion. HCT116 cells were treated with **13** at concentrations of 0.1, 0.2 and 0.3 μM for 24 h or 48 h. As shown in Fig. 4A&C, **13** inhibited cells migrating in a dose-dependent manner, compared with the control group which were treated with 0.1% DMSO. And in the assay of invasion, Compound **13** also could inhibit HCT116 cells penetration in a concentration-dependent manner, compared with the control group (0.1% DMSO) in Fig. 4B&D. These results indicated that compound **13** displayed strong ability to suppress HCT116 cells invasion and migration.

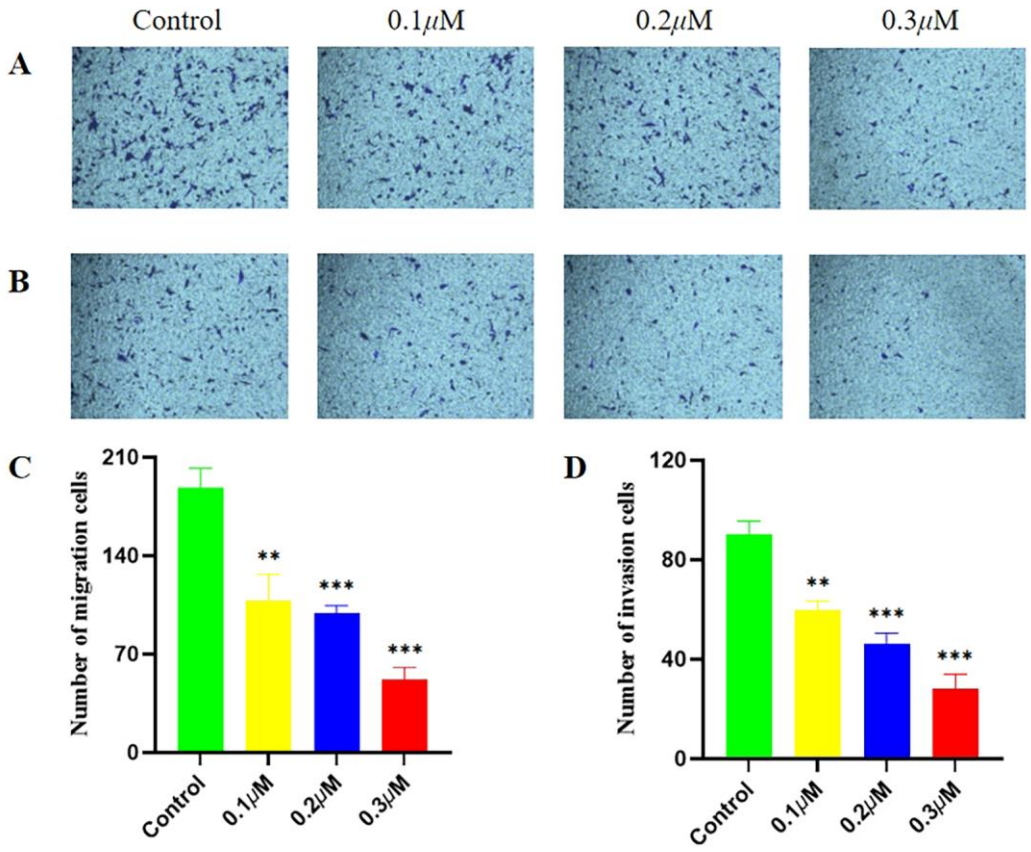

Fig. 4. Compound **13** inhibited the migration (A) and invasion (B) in HCT116 cells by Transwell assays. HCT116 cells were treated with different concentrations of **13** (0.1 μM, 0.2 μM and 0.3 μM) for 24

h in migration and 48 h in invasion, respectively. The relative migration (C) and invasion (D) numbers were shown in histograms. Data are presented as the mean ± SD, **: $p < 0.01$, ***: $p < 0.001$, compared with the control. At least three or more replicates.

2.4. Tubulin polymerization inhibition in vitro

As we know, as a tubulin polymerization inhibitor, CA-4 could effect on microtubules [38]. Fluorescent tubulin antibodies and confocal microscopy were used to detect the effects on the microtubule [39]. In order to further discuss whether compound **13** also has a similar function to CA-4, different concentrations of **13** (0.1, 0.2, and 0.3 μM) were added into HCT116 cells for 48 h, and control group were treated with 0.1% DMSO. As shown in (Fig. 5), the microtubule networks around the nucleus has been destroyed which HTC116 cells were treated with compound **13**, and high concentration of **13** showed stronger ability to inhibit tubulin polymerization, compared with the control group. These results shown that compound **13** has a significant inhibition on microtubule polymerization in HCT116 cells in a dose-dependent manner.

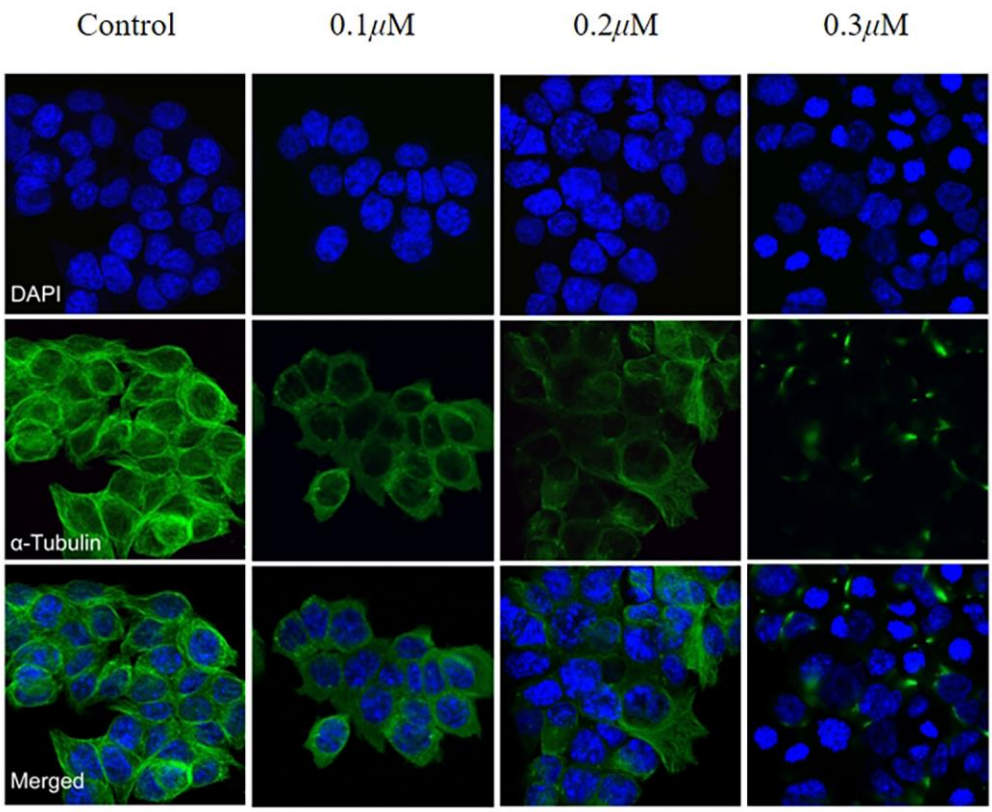

Fig. 5. Effects of compound **13** on the cellular microtubule networks in vitro. HCT116 cells were treated with 0.1 μM, 0.2 μM and 0.3 μM of compound **13** for 48 h, respectively. Blue represents the nucleus, green represents tubulin.

*2.5. Compound **13** blocks the cell cycle of HCT116 cells*

Cell cycle plays a fundamental role in cell life activity and cell proliferation could be effectively inhibited by blocking the cell cycle and inhibiting cell mitosis [40, 41]. The cell cycle progression assay was performed by treating HCT116 cells at various concentrations of **13** (0.1, 0.2, and 0.3 μM) for 24 h, respectively. As illustrated in (Fig. 6A&B), the cell cycle of HCT116 cells was significantly arrested at the G2/M phase, and the percentage of cells in the G2/M stage increased from 28.83% to 88.26% compared with the control group which the cells were incubated with 0.1% DMSO. These results indicated that **13** significantly induced cell cycle arrest at G2/M

phase in HCT116 cells. As we know, the characteristic of tubulin polymerization inhibitors is that they will arrest cells in the G2/M phase. Compound **13** arrests most cells in the G2/M cycle, which may indicate that it exerted anti-tumor effects through the inhibition of tubulin polymerization as we imagined.

*2.6. Compound **13** regulates the expression of cell-cycle-related proteins*

The complex of Cdc 2 and Cyclin B1 is important for regulating the G2 transition [42, 43]. Therefore, compound **13** was used to measure the expression levels of the cell-cycle-regulated proteins Cdc 2 and Cyclin B1 by Western blot. HCT116 cells were incubated with compound **13** at different concentrations (0.1, 0.2, and 0.3 μM) for 48 h and the control group were treated with 0.1% DMSO. As shown in (Fig. 6C&D), compound **13** could reduce the expression of Cdc 2 and Cyclin B1 in a dose-dependent manner. The results indicated that cell cycle arrest in HCT116 cells caused by compound **13** might associate the inhibition of the Cdc 2 and Cyclin B1 signaling pathway.

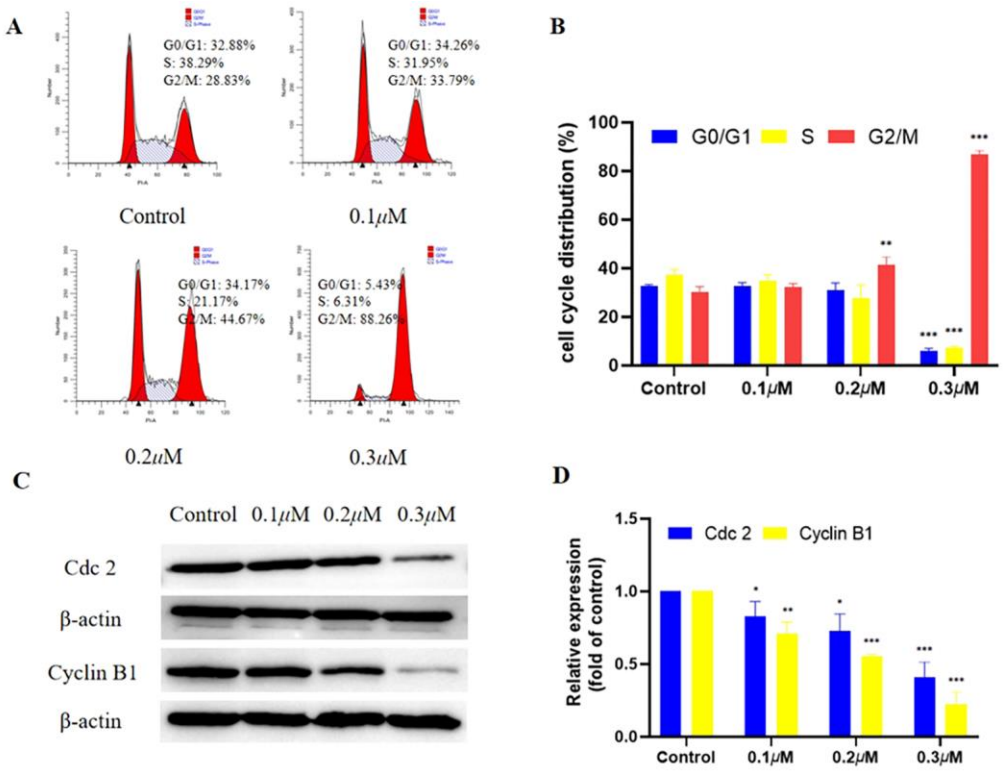

Fig. 6. Compound **13** induced G2/M phase arrest in HCT116 cells. (A) HCT116 cells were treated respectively with indicated concentrations of compound **13** (0.1 μM, 0.2 μM and 0.3 μM) for 24 h and analyzed by flow cytometry. (B) Histograms displayed the percentage of cell cycle distribution. (C) Western blot analyzed the levels of the G2/M-related proteins Cdc 2, Cyclin B1 in HCT116 cells after incubated respectively with different concentrations of compound **13** (0.1 μM, 0.2 μM and 0.3 μM) for 48 h. (D) Histograms displayed the quantification of related protein levels in (C) which the control group were set to 1. Data are represented as mean ± SD of three independent experiments. *: $p < 0.05$, **: $p < 0.01$, ***: $p < 0.001$, compared with the control group.

*2.7. Compound **13** activates autophagy of HCT116 cells*

Autophagy is a very critical process in cell evolution which degrades dysfunctional cells in a conservative manner, and suppresses neoplasms in the nascent stages of tumorigenesis [44, 45]. LC3 and p62 are the two most studied autophagy-related proteins currently, LC3-II is considered as a signal for autophagy occurring and p62

will be consumed in the autophagy [46]. In the process of using GFP-LC3, the iconic protein molecule LC3 has been marked on the inner membrane of the autophagosome [47]. Aggregated fluorescent spots do not form in cells where autophagy do not occur. However, the LC3 which has been labeled forms yellow dots as the merging of red (mRFP) and green (GFP) when autophagy occurs [48]. In our study, compound **13** was performed to investigate the changes of autophagy-related protein levels by Western blot. Treatment of HCT116 cells with compound **13** for 24 h resulted in the down-regulation of levels of p62 in a dose-dependent manner, and the expression of LC3-II increased significantly as the concentration of compound **13** increased (Fig. 7A&B). Additionally, HCT116 cells were treated with **13** at various concentrations (0.1, 0.2, and 0.3 μM) for 24 h after successful infection with mRFP-GFP-LC3 adenovirus (Fig. 7C). It could be known that the number of yellow dots became more which indicated autophagy occurs, as the concentration of **13** increased. These findings suggested that compound **13** might inhibit HCT116 cells proliferation by regulating the key autophagy-related proteins, which played crucially role in triggering autophagy.

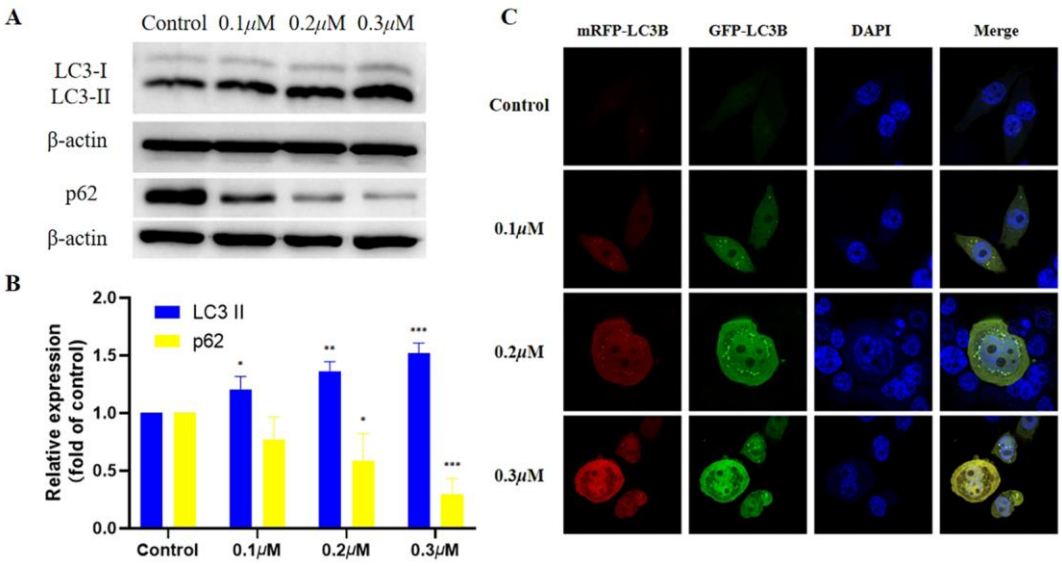

Fig. 7. Compound **13** induced autophagy in HCT116 cells. (A) The levels of the autophagy-related proteins LC3 II, p62 in HCT116 cells which after treatment with different concentrations of compound **13** (0.1 μM, 0.2 μM and 0.3 μM) for 24 h, were detected by Western blot respectively. (B) Histograms shown the conversion and decrease quantification of related protein levels in (A) which the control group were set to 1. (C) Confocal microscopy images of mRFP-GFP-LC3-HCT116 cells after treated respectively with varying concentrations of compound **13** (0.1 μM, 0.2 μM and 0.3 μM) for 24 h. Data are represented as mean ± SD of three independent experiments. *: $p < 0.05$, **: $p < 0.01$, ***: $p < 0.001$, compared with the control group.

*2.8. Compound **13** blocks the cell cycle and induces apoptosis of A549 cells*

The mechanism of inhibiting the proliferation of lung cancer cells has also been studied since compound **13** has good inhibitory activity against A549 cells. PI/RNase Staining Buffer, Annexin V-APC/PI Apoptosis Kit and flow cytometry analysis were used to estimate the effects on the cell cycle and apoptosis [40, 49]. Treatment of A549 cells with compound **13** (0.1 μM, 0.2 μM and 0.3 μM) for 24 h caused an accumulation of cells in the G0/G1 phase in a concentration-dependent manner. The percentage distributed at the G0/G1 stage was increased form 41.91% to 87.18%, compared with control group which were treated with 0.1% DMSO (Fig. 8A&B). And the total percentage of early apoptotic and late apoptotic cells was 13.12%, 22.15%, and 29.96% respectively, compared with the control group 2.59% (Fig. 8C&D). These results significantly demonstrated that **13** could exert anti-cancer effect by blocking cell cycle in the G0/G1 phase and inducing cell apoptosis in A549 cells.

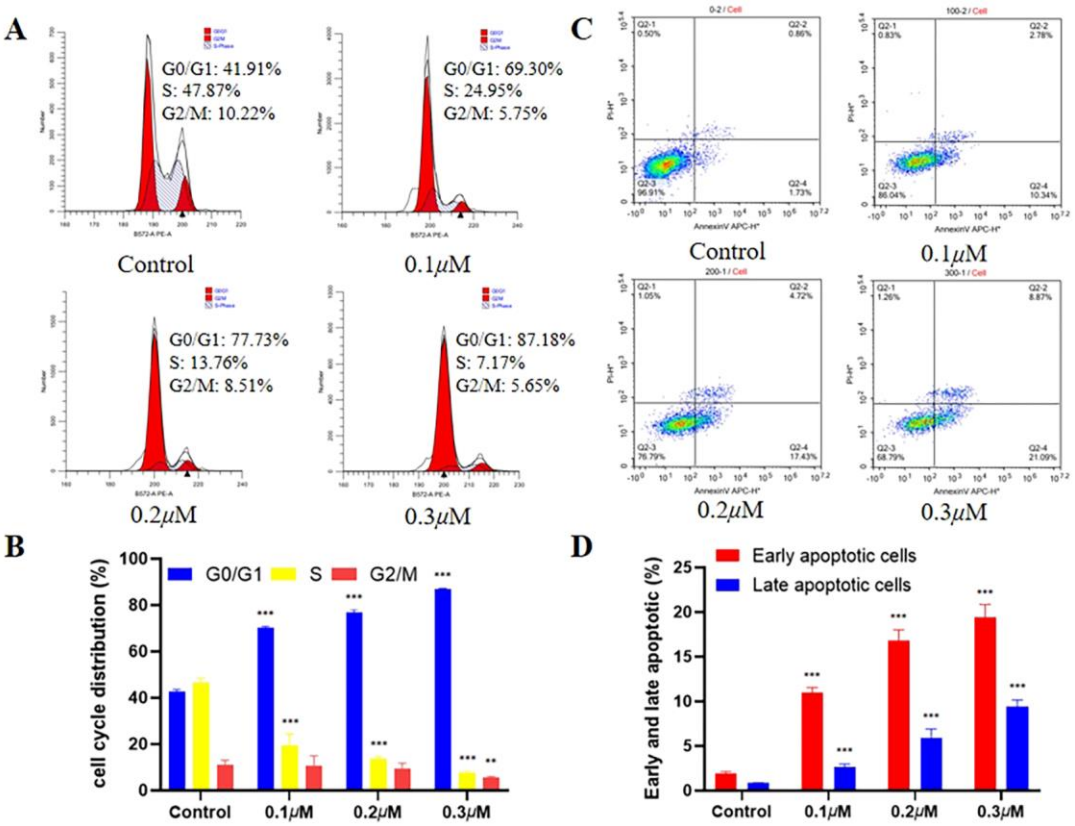

Fig. 8. Compound **13** induced G0/G1 phase arrest and apoptosis in A549 cells. (A) A549 cells were treated respectively with indicated concentrations of compound **13** (0.1 μM, 0.2 μM and 0.3 μM) for 24 h and analyzed by flow cytometry. (B) Histograms displayed the percentage of cell cycle distribution. (C) Different concentrations of compound **13** (0.1 μM, 0.2 μM and 0.3 μM) which incubated for 24 h induced apoptosis in A549 cells. (D) Histograms displayed the percentage of cell distribution. Data are represented as mean ± SD of three independent experiments. **: $p < 0.01$, ***: $p < 0.001$, compared with the control group.

2.9. In vivo antitumor efficacy

Encouraged by the significant anti-tumor cell proliferative activity in vitro of compound **13**, a colon cancer xenograft model by subcutaneous inoculation of HCT116 cells was established to evaluate **13** anticancer activity in vivo. HCT116 cells were injected into the right underarm (forelimb) of each mouse. Total of 40 mice were

randomly divided into 4 groups (ten mice per group) and received various treatments by intraperitoneal injection with control (saline), cisplatin (5mg/kg, every three days) and compound **13** (20 or 40 mg/kg, every two days) for 20 days. As illustrated in (Fig. 9A&B), the mice tumor volume and weight of nude mice were monitored during treatment days. Compound **13**, at a low dose of 20 mg/kg/2days only actualize the value of tumor growth inhibition (TGI) of 1.48%, compared with the control group. Importantly, the high dose of compound **13**-treated-group, 40 mg/kg/2days, achieved tumor growth inhibition (TGI) rate of 12.74%, while the cisplatin-treated-group achieved TGI rate of 33.28% at 5 mg/kg/3days. During the 20 days of treatment, none of the animals in the different treatment groups had any adverse effects and their body weight remained relatively stable, which suggests that **13** had low toxicity. At the end of the observation, the mice were euthanized and tumors were excised and weighed (Fig. 9C&D), the trend of tumor weight and tumor growth were consistent. In summary, these findings suggest that **13** could inhibit tumor growth in vivo without obvious toxicity, which has the potential to be a drug candidate for colon cancer.

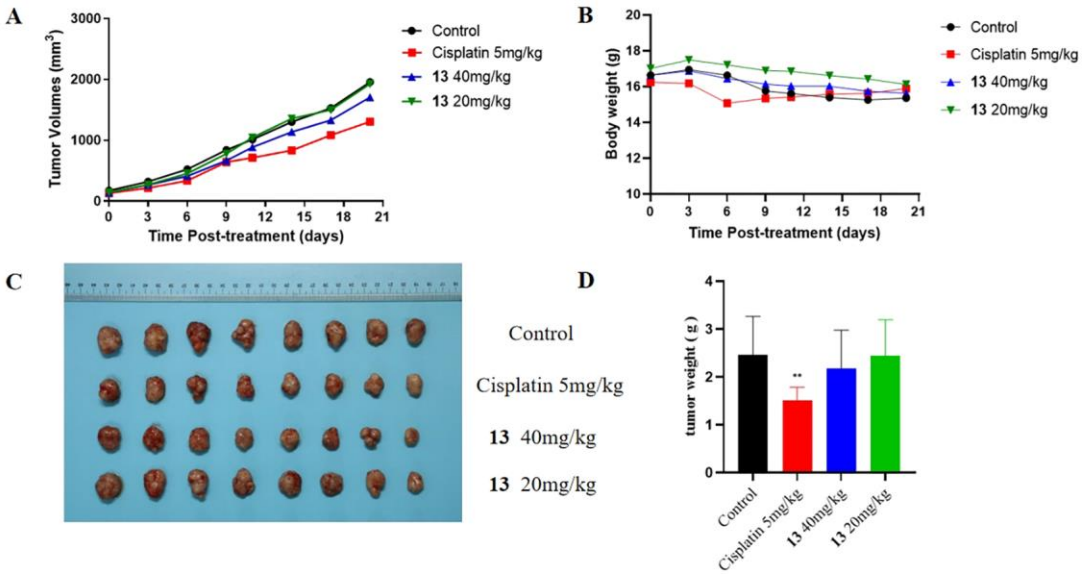

Fig. 9. Anti-tumor effects of **13** on HCT116 xenograft tumors growth in vivo. (A) Total of 40 mice were randomly divided into 4 groups, 10 mice in each group. Mice were treated intraperitoneally with control (saline), cisplatin (5mg/kg, every three days) and compound **13** (20 or 40 mg/kg, every two days) for 20 days. The curves of tumor growth in the different groups during treatment. (B) The curves of body weight of the HCT116 tumor-bearing mice in the four groups during treatment. (C) Photographs of the tumors removed from HCT116 tumor-bearing mice after treatment. (D) Histograms display the weight of the tumors in each isolated group. **: $p < 0.01$, compared with the control group.

2.10. Molecular modelling studies

To investigate the potential role of most valuable compound, **13** was performed the molecular modeling studies within the binding site of colchicine (PDB: 5LYJ) [50]. Docking simulations of the binding site of colchicine in tubulin show that the binding mode of **13** and CA-4 have much in common, they have formed a suitable steric complementarity with the binding site of Tubulin. The hydroxyl oxygen atoms of **13** and CA-4 are hydrogen bonding with Thrα179 in Tubulin-α, respectively. The residues that are spatially 4.5 Å away from **13** and CA-4, like Lysβ254, Lysβ352, Asnβ258, Leuβ255, etc., formed van der Waals interactions with **13** and CA-4 (Fig. 10A&B). It should be noted that some additional residues which as sidechain donor or backbone donor also interacted with **13**, such as Gluβ200, Pheβ169, this is a little different from CA-4. Collectively, there are many similarities between compound **13** and CA-4 in the binding of colchicine on tubulin. These similarities may make **13** to have a strong affinity for colchicine like CA-4, thereby exerting antitumor effects by acting as a tubulin polymerization inhibitor.

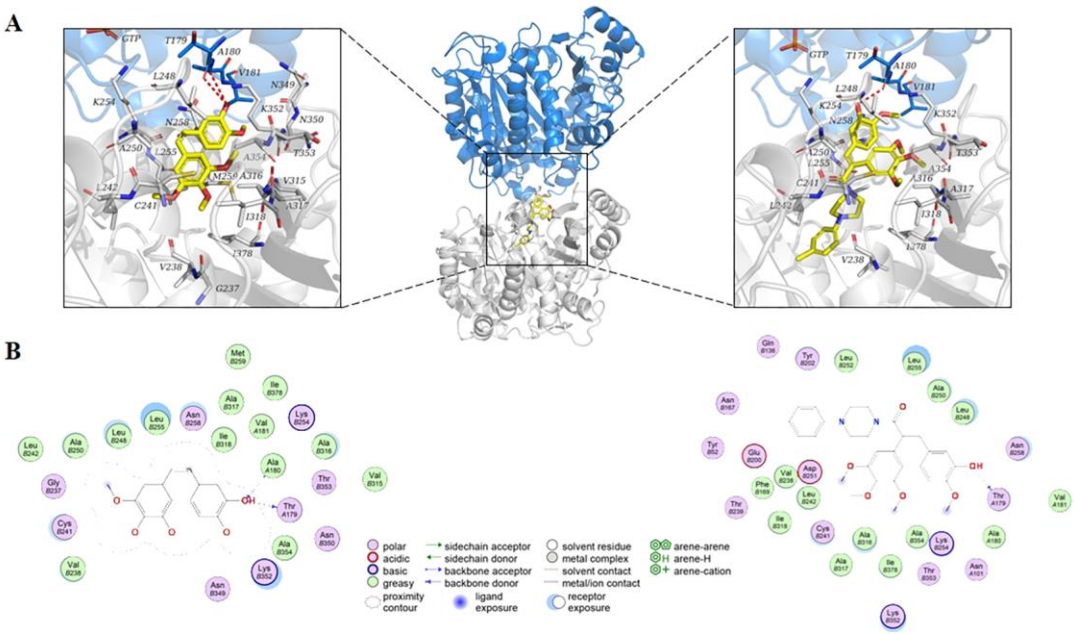

Fig. 10. Proposed binding models of CA-4 and compound **13** in tubulin (PDB: 5LYJ). (A) 3D binding model of compound and tubulin. The compound is colored in yellow. The tubulin-α is colored in marine and tubulin-β is colored in white. The residues in tubulin-α are shown as marine sticks and the residues in tubulin-β are shown as white sticks. The interactions are depicted as dashed lines. (B) 2D binding model of compound and tubulin. The legend has been given in the figure.

3. Conclusions

In conclusion, this study reports a series of novel compounds, some of which exhibited better anti-proliferative activity against tumor cells at lower concentrations. **13** inhibited proliferation of colon carcinoma HCT116 cells notably, but exhibited low toxicity to normal human colon mucosal epithelial cells (NCM460). Furthermore, we found that **13** could inhibit the invasion and migration of HCT116 tumor cells. In subsequent experiments, the results showed that **13** could effectively prevent tubulin polymerization at lower concentrations and destroy the tubulin grid structure around the nucleus. In mechanistic studies, **13** could make HCT116 tumor cells arrest in G2/M

phase by down-regulating the protein expression levels of Cyclin B1 and Cdc 2 and it could also induce autophagy in HCT116 cells by increasing the expression levels of LC3 II and reducing the expression levels of p62. Moreover, **13** could make A549 cells undergo cell cycle arrest and cell apoptosis. In addition, as a prodrug, the carbohydrate derivatives of compound **13** significantly improved its water solubility. Importantly, **13** effectively inhibited tumor growth in the HCT116 colon cancer xenograft mouse model *in vivo* in the absence of obvious signs of toxicity. These findings suggest that **13** is a promising candidate as a tubulin inhibitor for cancer treatment.

4. Experimental section

4.1. Chemistry

All chemicals and solvents were purchased from commercial suppliers as reagent grade quality or better, and were used without further purification. Thin layer chromatography (TLC) was performed on silica gel GF254 (Anhui Liang Chen Silicon Material Co. Ltd.). Column chromatography was carried out on silica gel (200-300 mesh, Shanghai Macklin Biochemical Technology Co., Ltd.). ^{1}H NMR, ^{13}C NMR and ^{19}F NMR spectra were recorded on Bruker spectrometer and Jeol spectrometer, respectively, with tetramethylsilane (TMS) as an internal standard and DMSO-d_6 or $CDCl_3$ as solvents. The chemical shifts were referenced relative to solvent peak, 2.50 ppm (^{1}H) and 39.52 ppm (^{13}C) for DMSO-d_6, 7.26 ppm (^{1}H) and 77.16 ppm (^{13}C) for $CDCl_3$ at 25°C. All chemical shifts are indicated in parts per million (ppm). All coupling constants (J) were described in hertz (Hz). ESIHRMS data were obtained on a Bruker Daltonics Apex-Ultra 7.0 T (Bruker Corporation, Billerica, MA, USA).

*4.1.1. Synthesis of (E)-3-(3-hydroxy-4-methoxyphenyl)-2-(3,4,5-trimethoxyphenyl) acrylic acid **(A)*** 3,4,5-Trimethoxyphenylacetic acid (1.91 g, 9 mmol, 1.0 eq) with 3-Hydroxy-4-methoxybenzaldehyde (1.37 g, 9 mmol, 1.0 eq) was refluxed for 6 h in the presence of triethylamine (5 mL) and acetic anhydride (10 mL). After acidification with concentrated hydrochloric acid (20 mL), the solid was dissolved in DCM (20 mL), washed with saturated $NaHCO_3$ solution and brine, dried over Na_2SO_4, and then concentrated. The residue was purified by silica gel chromatography (CH_2Cl_2/CH_3OH, 10:1) to yield the **A** as a yellow solid (1.36 g, 42%). ^{1}H NMR (400 MHz, DMSO-d_6, J in Hz) δ_H 12.44 (s, 1H), 8.96 (s, 1H), 7.58 (s, 1H), 6.80 (d, J = 8.4 Hz, 1H), 6.61 (dd, J = 8.4, 2.0 Hz, 1H), 6.54 (d, J = 2.0 Hz, 1H), 6.44 (s, 2H), 3.73 (s, 3H), 3.71 (s, 3H), 3.69 (s, 6H). ^{13}C NMR (100 MHz, DMSO-d_6) δ_C 168.57, 153.09, 148.90, 145.88, 139.09, 137.06, 132.13, 130.39, 127.08, 122.95, 117.22, 111.56, 106.85, 60.14, 55.97, 55.49. ESIHRMS *m/z* calcd for $C_{19}H_{20}O_7Na^+$ 383.1107 $[M+Na]^+$, found 383.1088.

*4.1.2. General method to synthesize **1-22***

The mixture of compound **A** (1 mmol)**,** EDCI (1 mmol) and HOBt (1 mmol) were dissolved in dry DCM (5 mL), and then added the DIPEA (2 mL) slowly. A series of nitrogen-containing heterocyclic compounds (1 mmol) and piperazine derivatives (1 mmol) were added in the mixture and stirred for 12 h at room temperature. The resulting mixture was dissolved in DCM (20 mL), washed with saturated $NaHCO_3$ solution and brine, dried over Na_2SO_4, and then concentrated. The residue was purified by silica gel chromatography to give the desired compound **1**-**22**.

4.1.2.1.(E)-3-(3-hydroxy-4-methoxyphenyl)-1-(pyrrolidin-1-yl)-2-(3,4,5-trimethoxyphenyl)prop-2-en-1-one ***(1)***. White solid (191 mg, 46%); ^{1}H NMR (400 MHz, $CDCl_3$, *J* in Hz) δ_H 6.75 (d, *J* = 1.6 Hz, 1H), 6.66 (s, 1H), 6.60 (s, 1H), 6.59 (dd, *J* = 8.4, 1.6 Hz, 1H), 6.53 (s, 2H), 3.81 (s, 3H), 3.78 (s, 3H), 3.66 (s, 6H), 3.50 (s, 2H), 3.25 (s, 2H), 1.81 (s, 4H). ^{13}C NMR (100 MHz, $CDCl_3$) δ_C 170.10, 153.33, 146.66, 145.34, 137.91, 136.94, 130.87, 130.77, 128.69, 121.93, 115.82, 110.37, 106.57, 60.96, 56.22, 55.90, 48.24, 46.09, 26.14, 24.33. ESIHRMS *m/z* calcd for $C_{23}H_{27}NO_6Na^+$ 436.1736 $[M+Na]^+$, found 436.1723.

4.1.2.2.(E)-3-(3-hydroxy-4-methoxyphenyl)-1-morpholino-2-(3,4,5-trimethoxyphenyl)prop-2-en-1-one ***(2)***. White solid (176 mg, 41%); ^{1}H NMR (400 MHz, $CDCl_3$, *J* in Hz) δ_H 6.74 (d, *J* = 0.8 Hz, 1H), 6.63 (s, 2H), 6.54 (s, 1H), 6.51 (s, 2H), 3.82 (s, 3H), 3.79 (s, 3H), 3.67 (s, 6H), 3.66-3.58 (m, 4H), 3.57 (s, 4H). ^{13}C NMR (100 MHz, $CDCl_3$) δ_C 170.53, 153.43, 146.72, 145.35, 138.16, 135.01, 130.70, 130.35, 128.37, 121.95, 115.62, 110.39, 106.21, 66.77, 60.96, 56.23, 55.93, 47.58, 42.54. ESIHRMS *m/z* calcd for $C_{23}H_{27}NO_7Na^+$ 452.1685 $[M+Na]^+$, found 452.1674.

4.1.2.3.(E)-3-(3-hydroxy-4-methoxyphenyl)-1-(piperazin-1-yl)-2-(3,4,5-trimethoxyphenyl)prop-2-en-1-one ***(3)***. White solid (151 mg, 35%); ^{1}H NMR (400 MHz, $CDCl_3$, *J* in Hz) δ_H 6.69 (d, *J* = 1.6 Hz, 1H), 6.64 (s, 1H), 6.63 (s, 1H), 6.53 (s, 2H), 6.50 (s, 1H), 3.81 (s, 3H), 3.79 (s, 3H), 3.67 (s, 6H), 3.66-3.59 (m, 4H), 3.58 (s, 2H), 3.57 (s, 2H), 2.75 (s, 2H), 2.73 (s, 2H). ^{13}C NMR (100 MHz, $CDCl_3$) δ_C 170.46, 153.42, 146.98, 145.53, 138.02, 135.16, 130.96, 129.95, 128.41, 121.94, 115.71, 110.53, 106.21,

60.98, 56.25, 55.92, 47.91, 45.77, 42.66. ESIHRMS *m/z* calcd for $C_{23}H_{28}N_2O_6Na^+$ 451.1845 $[M+Na]^+$, found 451.1834.

4.1.2.4.(E)-3-(3-hydroxy-4-methoxyphenyl)-1-thiomorpholino-2-(3,4,5-trimethoxyphenyl)prop-2-en-1-one ***(4)***. White solid (186 mg, 42%); ^{1}H NMR (400 MHz, $CDCl_3$, *J* in Hz) δ_H 6.74 (d, *J* = 1.2 Hz, 1H), 6.63 (s, 2H), 6.52 (s, 2H), 6.50 (s, 1H), 3.82 (s, 3H), 3.79 (s, 3H), 3.67 (s, 6H), 2.58 (s, 2H), 2.34 (s, 2H). ^{13}C NMR (100 MHz, $CDCl_3$) δ_C 170.60, 153.47, 146.66, 145.32, 138.20, 135.46, 130.59, 129.70, 128.37, 121.94, 115.57, 110.37, 106.22, 61.00, 56.27, 55.93, 49.71, 44.48, 27.47. ESIHRMS *m/z* calcd for $C_{23}H_{27}NO_6SNa^+$ 468.1457 $[M+Na]^+$, found 468.1447.

4.1.2.5.(E)-1-(1,1-dioxidothiomorpholino)-3-(3-hydroxy-4-methoxyphenyl)-2-(3,4,5-trimethoxyphenyl)prop-2-en-1-one ***(5)***. White solid (209 mg, 44%); ^{1}H NMR (400 MHz, $CDCl_3$, *J* in Hz) δ_H 6.74 (d, *J* = 1.6 Hz, 1H), 6.66 (d, *J* = 8.4 Hz, 1H), 6.64 (d, *J* = 1.6 Hz, 1H), 6.63 (s, 1H), 6.50 (s, 2H), 4.04 (s, 4H), 3.84 (s, 3H), 3.82 (s, 3H), 3.68 (s, 6H), 2.87 (d, *J* = 1.6 Hz, 4H). ^{13}C NMR (100 MHz, $CDCl_3$) δ_C 170.78, 153.80, 147.02, 145.37, 138.63, 134.03, 131.34, 130.02, 127.77, 122.29, 115.58, 110.42, 106.11, 61.09, 56.40, 55.98, 51.86, 45.67, 39.96. ESIHRMS *m/z* calcd for $C_{23}H_{27}NO_8SNa^+$ 500.1355 $[M+Na]^+$, found 500.1342.

4.1.2.6.(E)-1-(4-(2-fluorophenyl)piperazin-1-yl)-3-(3-hydroxy-4-methoxyphenyl)-2-(3,4,5-trimethoxyphenyl)prop-2-en-1-one ***(6)***. White solid (245 mg, 47%); ^{1}H NMR (600 MHz, $CDCl_3$, *J* in Hz) δ_H 7.06-7.03 (m, 1H), 7.03-6.99 (m, 1H), 6.98-6.95 (m, 1H), 6.90 (t, *J* = 8.1 Hz, 1H), 6.80 (s, 1H), 6.67 (s, 2H), 6.60 (s, 1H), 6.58 (s, 2H), 5.71 (s, 1H), 3.88-3.68 (m, 4H), 3.85 (s, 3H), 3.84 (s, 3H), 3.71 (s, 6H), 3.08 (s, 2H), 2.91

(s, 2H). ^{13}C NMR (150 MHz, $CDCl_3$) δ_C 170.52, 156.65 (d, $^1J_{C\text{-}F}$ = 244.9 Hz), 155.02, 153.48, 146.62, 145.31, 139.47 (d, $^3J_{C\text{-}F}$ = 7.4 Hz), 139.42, 138.09, 135.38, 130.90, 130.20, 128.53, 124.69 (d, $^4J_{C\text{-}F}$ = 2.6 Hz), 124.67, 123.45 (d, $^3J_{C\text{-}F}$ = 7.0 Hz), 123.40, 122.07, 119.40, 116.45 (d, $^2J_{C\text{-}F}$ = 20.6 Hz), 116.32, 115.61, 110.35, 106.18, 61.07, 56.29, 56.00, 51.00, 50.54, 47.23, 42.09. ESIHRMS *m/z* calcd for $C_{29}H_{31}FN_2O_6Na^+$ 545.2064 $[M+Na]^+$, found 545.2045.

4.1.2.7.(E)-1-(4-(4-fluorophenyl)piperazin-1-yl)-3-(3-hydroxy-4-methoxyphenyl)-2-(3,4,5-trimethoxyphenyl)prop-2-en-1-one ***(7)***. White solid (213 mg, 41%); ^{1}H NMR (600 MHz, $CDCl_3$, *J* in Hz) δ_H 6.97-6.95 (m, 1H), 6.94 (s, 1H), 6.85 (d, *J* = 4.5 Hz, 1H), 6.83 (d, *J* = 4.5 Hz, 1H), 6.79 (s, 1H), 6.67 (s, 2H), 6.60 (s, 1H), 6.57 (s, 2H), 5.74 (s, 1H), 3.88-3.68(m, 4H), 3.85 (s, 3H), 3.83 (s, 3H), 3.70 (s, 6H), 3.08 (s, 2H), 2.92 (s, 2H). ^{13}C NMR (150 MHz, $CDCl_3$) δ_C 170.49, 158.54 (d, $^1J_{C\text{-}F}$ = 238.6 Hz), 156.95, 153.48, 147.58, 146.64, 145.31, 138.11, 135.31, 130.86, 130.30, 128.49, 122.08, 118.74 (d, $^3J_{C\text{-}F}$ = 7.4 Hz), 118.69, 115.88 (d, $^2J_{C\text{-}F}$ = 21.8 Hz), 115.74, 115.61, 110.35, 106.19, 61.07, 56.29, 55.99, 50.73, 50.67, 47.08, 42.01. ESIHRMS *m/z* calcd for $C_{29}H_{31}FN_2O_6Na^+$ 545.2064 $[M+Na]^+$, found 545.2046.

4.1.2.8.(E)-1-(4-(2-chlorophenyl)piperazin-1-yl)-3-(3-hydroxy-4-methoxyphenyl)-2-(3,4,5-trimethoxyphenyl)prop-2-en-1-one ***(8)***. White solid (215 mg, 40%); ^{1}H NMR (600 MHz, $CDCl_3$, *J* in Hz) δ_H 7.35 (dd, *J* = 8.4, 1.2 Hz, 1H), 7.22-7.19 (m, 1H), 7.00 (d, *J* = 7.8 Hz, 1H), 6.97 (d, *J* = 10.2 Hz, 1H), 6.80 (s, 1H), 6.67 (s, 2H), 6.60 (s, 1H), 6.58 (s, 2H), 5.70 (s, 1H), 3.88-3.68(m, 4H), 3.86 (s, 3H), 3.84 (s, 3H), 3.71 (s, 6H), 3.05 (s, 2H), 2.88 (s, 2H). ^{13}C NMR (150 MHz, $CDCl_3$) δ_C 170.59, 153.47, 148.60,

146.59, 145.31, 138.09, 135.48, 130.93, 130.84, 130.07, 128.99, 128.57, 127.81, 124.46, 122.06, 120.66, 115.61, 110.35, 106.20, 61.08, 56.30, 56.00, 51.65, 51.20, 47.44, 42.24. ESIHRMS *m/z* calcd for $C_{29}H_{31}ClN_2O_6Na^+$ 561.1768 $[M+Na]^+$, found 561.1747.

4.1.2.9.(E)-1-(4-(4-chlorophenyl)piperazin-1-yl)-3-(3-hydroxy-4-methoxyphenyl)-2-(3,4,5-trimethoxyphenyl)prop-2-en-1-one ***(9)***. White solid (227 mg, 42%); ^{1}H NMR (600 MHz, $CDCl_3$, *J* in Hz) δ_H 7.20 (s, 1H), 7.19 (s, 1H), 6.81 (s, 1H), 6.79 (s, 2H), 6.67 (s, 1H), 6.67 (s, 1H), 6.60 (s, 1H), 6.57 (s, 2H), 5.69 (s, 1H), 3.88-3.68(m, 4H), 3.85 (s, 3H), 3.84 (s, 3H), 3.70 (s, 6H), 3.12 (s, 2H), 2.97 (s, 2H). ^{13}C NMR (150 MHz, $CDCl_3$) δ_C 170.50, 153.50, 149.53, 146.65, 145.31, 138.14, 135.28, 130.83, 130.40, 129.21, 128.47, 125.63, 122.10, 117.99, 115.60, 110.35, 106.20, 61.08, 56.30, 56.00, 49.69, 46.81, 41.85. ESIHRMS *m/z* calcd for $C_{29}H_{31}ClN_2O_6Na^+$ 561.1768 $[M+Na]^+$, found 561.1752.

4.1.2.10.(E)-1-(4-(4-bromophenyl)piperazin-1-yl)-3-(3-hydroxy-4-methoxyphenyl)-2-(3,4,5-trimethoxyphenyl)prop-2-en-1-one ***(10)***. White solid (256 mg, 44%); ^{1}H NMR (600 MHz, $CDCl_3$, *J* in Hz) δ_H 7.34 (d, *J* = 2.4 Hz, 1H), 7.33 (d, *J* = 1.8 Hz, 1H), 6.79 (s, 1H), 6.76 (s, 1H), 6.74 (s, 1H), 6.67 (s, 2H), 6.60 (s, 1H), 6.56 (s, 2H), 5.69 (s, 1H), 3.88-3.68(m, 4H), 3.85 (s, 3H), 3.84 (s, 3H), 3.70 (s, 6H), 3.13 (s, 2H), 2.97 (s, 2H). ^{13}C NMR (150 MHz, $CDCl_3$) δ_C 170.50, 153.50, 149.90, 146.65, 145.31, 138.14, 135.26, 132.14, 130.82, 130.42, 128.46, 122.11, 118.36, 115.59, 112.97, 110.34, 106.19, 61.08, 56.31, 56.00, 49.53, 46.77, 41.75. ESIHRMS *m/z* calcd for $C_{29}H_{31}BrN_2O_6Na^+$ 607.1243 $[M+Na]^+$, found 607.1226.

4.1.2.11.(E)-3-(3-hydroxy-4-methoxyphenyl)-1-(4-(o-tolyl)piperazin-1-yl)-2-(3,4,5-trimethoxyphenyl)prop-2-en-1-one ***(11)***. White solid (213 mg, 41%); ^{1}H NMR (400 MHz, $CDCl_3$, *J* in Hz) δ_H 7.18 (d, *J* = 7.0 Hz, 1H), 7.14 (d, *J* = 7.8 Hz, 1H), 7.00 (dt, *J* = 7.4, 3.6 Hz, 1H), 6.93 (d, *J* = 7.2 Hz, 1H), 6.81 (s, 1H), 6.68 (s, 2H), 6.60 (s, 1H), 6.60 (s, 2H), 5.76 (s, 1H), 3.88-3.68 (m, 4H), 3.86 (s, 3H), 3.84 (s, 3H), 3.72 (s, 6H), 2.89 (s, 2H), 2.76 (s, 2H), 2.30 (s, 3H). ^{13}C NMR (100 MHz, $CDCl_3$) δ_C 170.57, 153.47, 150.88, 146.60, 145.35, 138.14, 135.56, 132.77, 131.28, 130.95, 129.97, 128.63, 126.78, 123.89, 122.01, 119.23, 115.63, 110.38, 106.28, 61.05, 56.30, 55.99, 51.99, 47.67, 42.55, 17.88. ESIHRMS *m/z* calcd for $C_{30}H_{34}N_2O_6Na^+$ 541.2315 $[M+Na]^+$, found 541.2297.

4.1.2.12.(E)-3-(3-hydroxy-4-methoxyphenyl)-1-(4-(m-tolyl)piperazin-1-yl)-2-(3,4,5-trimethoxyphenyl)prop-2-en-1-one ***(12)***. White solid (222 mg, 43%); ^{1}H NMR (600 MHz, $CDCl_3$, *J* in Hz) δ_H 7.15 (t, *J* = 7.8 Hz, 1H), 6.80 (s, 1H), 6.72 (s, 1H), 6.71 (s, 1H), 6.69 (s, 1H), 6.68 (s, 2H), 6.61 (s, 1H), 6.58 (s, 2H), 5.76 (s, 1H), 3.88-3.68 (m, 4H), 3.85 (s, 3H), 3.84 (s, 3H), 3.70 (s, 6H), 3.18 (s, 2H), 2.99 (s, 2H), 2.30 (s, 3H). ^{13}C NMR (150 MHz, $CDCl_3$) δ_C 170.46, 153.45, 151.00, 146.61, 145.31, 139.08, 138.08, 135.39, 130.88, 130.24, 129.16, 128.53, 122.05, 121.60, 117.61, 115.62, 113.88, 110.34, 106.17, 61.05, 56.27, 55.98, 49.77, 47.03, 42.02, 21.79. ESIHRMS *m/z* calcd for $C_{30}H_{34}N_2O_6Na^+$ 541.2315 $[M+Na]^+$, found 541.2296.

4.1.2.13.(E)-3-(3-hydroxy-4-methoxyphenyl)-1-(4-(p-tolyl)piperazin-1-yl)-2-(3,4,5-trimethoxyphenyl)prop-2-en-1-one ***(13)***. White solid (219 mg, 42%); ^{1}H NMR (400 MHz, $CDCl_3$, *J* in Hz) δ_H 7.08 (s, 1H), 7.06 (s, 1H), 6.81 (s, 1H), 6.80 (s, 1H), 6.79 (s,

1H), 6.67 (s, 1H), 6.67 (s, 1H), 6.60 (s, 1H), 6.58 (s, 2H), 5.84 (s, 1H), 3.88-3.68 (m, 4H), 3.85 (s, 3H), 3.83 (s, 3H), 3.70 (s, 6H), 3.09 (s, 2H), 2.97 (s, 2H), 2.26 (s, 3H). ^{13}C NMR (100 MHz, $CDCl_3$) δ_C 170.46, 153.45, 148.85, 146.65, 145.36, 138.16, 135.39, 130.88, 130.29, 130.19, 129.83, 128.56, 122.01, 117.09, 115.64, 110.39, 106.27, 61.02, 56.27, 55.97, 50.24, 47.17, 41.94, 20.49. ESIHRMS *m/z* calcd for $C_{30}H_{34}N_2O_6Na^+$ 541.2315 $[M+Na]^+$, found 541.2300. Mp (142℃-144℃, MeOH).

4.1.2.14.(E)-3-(3-hydroxy-4-methoxyphenyl)-1-(4-(3-methoxyphenyl)piperazin-1-yl)-2-(3,4,5-trimethoxyphenyl)prop-2-en-1-one ***(14)***. White solid (231 mg, 43%); ^{1}H NMR (600 MHz, $CDCl_3$, *J* in Hz) δ_H 7.17 (t, *J* = 8.4 Hz, 1H), 6.79 (s, 1H), 6.68 (s, 2H), 6.60 (s, 1H), 6.57 (s, 2H), 6.50 (dd, *J* = 8.4, 1.2 Hz, 1H), 6.46-6.44 (m, 1H), 6.43 (s, 1H), 5.68 (s, 1H), 3.88-3.68 (m, 4H), 3.85 (s, 3H), 3.84 (s, 3H), 3.77 (s, 3H), 3.70 (s, 6H), 3.18 (s, 2H), 3.01 (s, 2H). ^{13}C NMR (150 MHz, $CDCl_3$) δ_C 170.49, 160.72, 153.48, 152.27, 146.62, 145.31, 138.11, 135.36, 130.87, 130.28, 130.06, 128.52, 122.10, 115.60, 110.35, 109.41, 106.18, 105.40, 103.27, 61.08, 56.29, 56.00, 55.32, 49.61, 46.95, 41.90. ESIHRMS *m/z* calcd for $C_{30}H_{34}N_2O_7Na^+$ 557.2264 $[M+Na]^+$, found 557.2242.

4.1.2.15.(E)-3-(3-hydroxy-4-methoxyphenyl)-1-(4-(4-methoxyphenyl)piperazin-1-yl)-2-(3,4,5-trimethoxyphenyl)prop-2-en-1-one ***(15)***. White solid (237 mg, 44%); ^{1}H NMR (400 MHz, $CDCl_3$, *J* in Hz) δ_H 6.87-6.84 (m, 1H), 6.84 (s, 1H), 6.83 (s, 1H), 6.83-6.80 (m, 1H), 6.79 (s, 1H), 6.67 (s, 1H), 6.67 (s, 1H), 6.59 (s, 1H), 6.57 (s, 2H), 5.82 (s, 1H), 3.88-3.68 (m, 4H), 3.84 (s, 3H), 3.82 (s, 3H), 3.75 (s, 3H), 3.70 (s, 6H), 3.03 (s, 2H), 2.90 (s, 2H). ^{13}C NMR (100 MHz, $CDCl_3$) δ_C 170.46, 154.51, 153.45, 146.63, 145.34, 145.26, 138.13, 135.39, 130.89, 130.16, 128.55, 122.02, 118.97, 115.63, 114.62,

110.37, 106.24, 61.04, 56.27, 55.97, 55.63, 51.16, 47.25, 42.19. ESIHRMS *m/z* calcd for $C_{30}H_{34}N_2O_7Na^+$ 557.2264 $[M+Na]^+$, found 557.2244.

4.1.2.16.(E)-3-(3-hydroxy-4-methoxyphenyl)-1-(4-(4-nitrophenyl)piperazin-1-yl)-2-(3,4,5-trimethoxyphenyl)prop-2-en-1-one ***(16)***. Yellow solid (227 mg, 41%); ^{1}H NMR (400 MHz, $CDCl_3$, *J* in Hz) δ_H 8.06 (d, *J* = 1.8 Hz, 1H), 8.04 (d, *J* = 2.0 Hz, 1H), 6.77 (s, 1H), 6.76 (s, 1H), 6.75-6.73 (m, 1H), 6.66 (s, 1H), 6.66 (s, 1H), 6.62 (s, 1H), 6.55 (s, 2H), 5.86 (s, 1H), 3.88-3.68 (m, 4H), 3.82 (s, 3H), 3.81 (s, 3H), 3.68 (s, 6H), 3.35 (s, 2H), 3.32 (s, 2H). ^{13}C NMR (100 MHz, $CDCl_3$) δ_C 170.67, 154.41, 153.49, 146.79, 145.31, 139.01, 138.17, 134.89, 130.87, 130.61, 128.19, 125.93, 122.11, 115.57, 113.06, 110.36, 106.17, 61.00, 56.27, 55.95, 47.01, 45.92, 41.51. ESIHRMS *m/z* calcd for $C_{29}H_{31}N_3O_8Na^+$ 572.2009 $[M+Na]^+$, found 572.2001.

4.1.2.17.(E)-4-(4-(3-(3-hydroxy-4-methoxyphenyl)-2-(3,4,5-trimethoxyphenyl)acryloyl)piperazin-1-yl)benzonitrile ***(17)***. White solid (223 mg, 42%); ^{1}H NMR (400 MHz, $CDCl_3$, *J* in Hz) δ_H 7.47 (s, 1H), 7.45 (s, 1H), 6.81 (s, 1H), 6.79 (s, 1H), 6.77 (s, 1H), 6.66 (s, 1H), 6.66 (s, 1H), 6.60 (s, 1H), 6.55 (s, 2H), 5.85 (s, 1H), 3.88-3.68 (m, 4H), 3.83 (s, 3H), 3.82 (s, 3H), 3.68 (s, 6H), 3.25 (s, 2H), 3.21 (s, 2H). ^{13}C NMR (100 MHz, $CDCl_3$) δ_C 170.58, 153.47, 152.95, 146.75, 145.31, 138.15, 134.97, 133.59, 130.70, 130.64, 128.23, 122.06, 119.74, 115.57, 114.66, 110.35, 106.17, 101.18, 60.99, 56.25, 55.94, 47.30, 46.41, 41.54. ESIHRMS *m/z* calcd for $C_{30}H_{31}N_3O_6Na^+$ 552.2111 $[M+Na]^+$, found 552.2105.

4.1.2.18.(E)-1-(4-(4-fluorobenzyl)piperazin-1-yl)-3-(3-hydroxy-4-methoxyphenyl)-2-(3,4,5-trimethoxyphenyl)prop-2-en-1-one ***(18)***. White solid (232 mg, 43%); ^{1}H NMR

(400 MHz, $CDCl_3$, *J* in Hz) δ_H 7.24 (d, *J* = 5.6 Hz, 1H), 7.22 (d, *J* = 5.6 Hz, 1H), 6.99 (s, 1H), 6.95 (s, 1H), 6.76 (s, 1H), 6.64 (s, 2H), 6.53 (s, 1H), 6.52 (s, 2H), 3.83 (s, 3H), 3.80 (s, 3H), 3.76-3.60 (m, 2H), 3.67 (s, 6H), 3.52 (s, 2H), 3.44 (s, 2H), 2.42 (s, 2H), 2.24 (s, 2H). ^{13}C NMR (100 MHz, $CDCl_3$) δ_C 170.39, 163.42 (d, $^1J_{C-F}$ = 243.9 Hz), 160.98, 153.39, 146.64, 145.34, 138.07, 135.48, 133.06, 130.90, 130.74 (d, $^3J_{C-F}$ = 7.9 Hz), 130.66, 129.94, 128.58, 121.94, 115.67, 115.33 (d, $^2J_{C-F}$ = 21.1 Hz), 115.12, 110.39, 106.24, 62.04, 61.01, 56.23, 55.95, 52.81, 47.06, 41.88. ESIHRMS *m/z* calcd for $C_{30}H_{33}FN_2O_6Na^+$ 559.2220 $[M+Na]^+$, found 559.2202.

4.1.2.19.(E)-1-(4-(4-chlorobenzyl)piperazin-1-yl)-3-(3-hydroxy-4-methoxyphenyl)-2-(3,4,5-trimethoxyphenyl)prop-2-en-1-one ***(19)***. White solid (243 mg, 44%); ^1H NMR (400 MHz, $CDCl_3$, *J* in Hz) δ_H 7.24 (s, 1H), 7.22 (s, 1H), 7.19 (s, 1H), 7.17 (s, 1H), 6.74 (s, 1H), 6.62 (s, 1H), 6.62 (s, 1H), 6.51 (s, 1H), 6.50 (s, 2H), 3.81 (s, 3H), 3.76 (s, 3H), 3.70-3.63 (m, 2H), 3.65 (s, 6H), 3.50 (s, 2H), 3.41 (s, 2H), 2.39 (s, 2H), 2.22 (s, 2H). ^{13}C NMR (100 MHz, $CDCl_3$) δ_C 170.35, 153.29, 146.68, 145.33, 137.97, 135.89, 135.29, 133.01, 130.81, 130.39, 129.91, 128.45, 121.82, 115.69, 110.39, 106.16, 61.97, 60.92, 56.14, 55.85, 52.74, 46.97, 41.85. ESIHRMS *m/z* calcd for $C_{30}H_{33}ClN_2O_6Na^+$ 575.1925 $[M+Na]^+$, found 575.1907.

4.1.2.20.(E)-3-(3-hydroxy-4-methoxyphenyl)-1-(4-(2-methylbenzyl)piperazin-1-yl)-2-(3,4,5-trimethoxyphenyl)prop-2-en-1-one ***(20)***. White solid (224 mg, 42%); ^1H NMR (400 MHz, $CDCl_3$, *J* in Hz) δ_H 7.20 (d, *J* = 7.2 Hz, 1H), 7.17-7.14 (m, 1H), 7.14 (s, 1H), 7.12 (dd, *J* = 6.8, 2.4 Hz, 1H), 6.78 (s, 1H), 6.66 (s, 1H), 6.65 (s, 1H), 6.55 (s, 1H), 6.54 (s, 2H), 5.80 (s, 1H), 3.85 (s, 3H), 3.82 (s, 3H), 3.75-3.64 (m, 2H), 3.69 (s, 6H), 3.51

(s, 2H), 3.44 (s, 2H), 2.45 (s, 2H), 2.34 (s, 3H), 2.28 (s, 2H). ^{13}C NMR (100 MHz, $CDCl_3$) δ_C 170.36, 153.41, 146.56, 145.32, 138.05, 137.63, 135.72, 135.64, 130.97, 130.47, 129.98, 129.82, 128.67, 127.42, 125.64, 121.96, 115.63, 110.36, 106.24, 61.04, 60.80, 56.26, 55.98, 53.04, 47.15, 42.05, 19.29. ESIHRMS *m/z* calcd for $C_{31}H_{36}N_2O_6Na^+$ 555.2471 $[M+Na]^+$, found 555.2453.

4.1.2.21.(E)-3-(3-hydroxy-4-methoxyphenyl)-1-(4-(3-methylbenzyl)piperazin-1-yl)-2-(3,4,5-trimethoxyphenyl)prop-2-en-1-one ***(21)***. White solid (235 mg, 44%); ^{1}H NMR (600 MHz, $CDCl_3$, *J* in Hz) δ_H 7.18 (t, *J* = 7.6 Hz, 1H), 7.08 (s, 1H), 7.06 (s, 1H), 7.05 (s, 1H), 6.77 (s, 1H), 6.65 (s, 2H), 6.54 (s, 1H), 6.53 (s, 2H), 5.90 (s, 1H), 3.84 (s, 3H), 3.81 (s, 3H), 3.75-3.64 (m, 2H), 3.68 (s, 6H), 3.52 (s, 2H), 3.44 (s, 2H), 2.45 (s, 2H), 2.32 (s, 3H), 2.26 (s, 2H). ^{13}C NMR (150 MHz, $CDCl_3$) δ_C 170.37, 153.37, 146.57, 145.30, 138.03, 137.96, 137.31, 135.55, 130.95, 129.97, 129.86, 128.61, 128.27, 128.13, 126.32, 121.94, 115.66, 110.34, 106.15, 62.96, 61.03, 56.22, 55.95, 53.03, 52.88, 47.10, 41.94, 21.45. ESIHRMS *m/z* calcd for $C_{31}H_{36}N_2O_6Na^+$ 555.2471 $[M+Na]^+$, found 555.2452.

4.1.2.22.(E)-3-(3-hydroxy-4-methoxyphenyl)-1-(4-(4-methylbenzyl)piperazin-1-yl)-2-(3,4,5-trimethoxyphenyl)prop-2-en-1-one ***(22)***. White solid (226 mg, 42%); ^{1}H NMR (600 MHz, $CDCl_3$, *J* in Hz) δ_H 7.16 (s, 1H), 7.15 (s, 1H), 7.11 (s, 1H), 7.10 (s, 1H), 6.77 (s, 1H), 6.65 (s, 2H), 6.54 (s, 1H), 6.52 (s, 2H), 5.83 (s, 1H), 3.85 (s, 3H), 3.82 (s, 3H), 3.75-3.64 (m, 2H), 3.68 (s, 6H), 3.52 (s, 2H), 3.45 (s, 2H), 2.44 (s, 2H), 2.32 (s, 3H), 2.26 (s, 2H). ^{13}C NMR (150 MHz, $CDCl_3$) δ_C 170.36, 153.38, 146.56, 145.29, 137.97, 137.07, 135.58, 134.24, 130.96, 129.86, 129.24, 129.10, 128.64, 121.97, 115.64,

110.33, 106.15, 62.65, 61.05, 56.22, 55.97, 52.98, 52.74, 47.11, 41.97, 21.19. ESIHRMS *m/z* calcd for $C_{31}H_{36}N_2O_6Na^+$ 555.2471 $[M+Na]^+$, found 555.2451.

*4.1.3. Preparation of Compound **31***

(2R,3S,4S,5R,6R)-6-(acetoxymethyl)tetrahydro-2H-pyran-2,3,4,5-tetrayl tetraacetate (5.0 g, 12.8 mmol) dissolved in THF (40 mL) and stirred overnight at room temperature with benzylamine (4.6 mL, 42 mmol). The mixture was purified by silica gel chromatography (EtOAc/petroleum ether, 1:1) to yield the intermediate **30**. And then the **30** (626 mg, 1.8 mmol) dissolved in DCM, DBU (0.14 mL, 0.9 mmol) and CCl_3CN (1.12 mL, 11.1 mmol) were added slowly under an inert atmosphere, compound **31** was given by stirring overnight at room temperature. After acidification with 1 mol/L HCl, the liquid was dissolved in DCM (20 mL), washed with saturated $NaHCO_3$ solution and brine, dried over Na_2SO_4, and then concentrated. The residue was purified by silica gel chromatography (EtOAc/n-hexane, 1:1) to yield the compound **31**.

*4.1.3.1.(2R,3R,4S,5S,6R)-2-(acetoxymethyl)-6-(2,2,2-trichloro-1-iminoethoxy)tetrahydro-2H-pyran-3,4,5-triyl triacetate **(31)***. Yellow solid (683 mg, 77%); ^{1}H NMR (400 MHz, $CDCl_3$, *J* in Hz) δ_H 8.78 (s, 1H), 6.24 (d, *J* = 1.8 Hz, 1H), 5.43 (t, *J* = 2.4 Hz, 1H), 5.37 (d, *J* = 1.6 Hz, 1H), 5.36 (d, *J* = 2.4 Hz, 1H), 4.26-4.22 (m, 1H), 4.16 (d, *J* = 6.0 Hz, 1H), 4.12 (d, *J* = 2.4 Hz, 1H), 2.17 (s, 3H), 2.05 (s, 3H), 2.04 (s, 3H), 1.98 (s, 3H). ^{13}C NMR (100 MHz, $CDCl_3$) δ_C 170.67, 169.90, 169.81, 169.72, 159.85, 94.61, 90.59, 71.30, 68.90, 67.96, 65.53, 62.15, 20.79, 20.71, 20.63.

*4.1.4. General method to synthesize **32-34***

To the mixture of compound **13** (259 mg, 0.5 mmol), TBAF (130 mg, 0.5 mmol) dissolved in DCM (10 mL), and then K_2CO_3 (550mg, 4mmol) were added. After stirring for 20 min, the donor **27-29** (0.8 mmol) was added slowly, respectively. And then the mixture of two phase reaction was stirred for 12 h, the residue was purified by silica gel column chromatography to give the desired products **32-34**.

4.1.4.1.(2S,3S,4R,5S,6R)-2-(acetoxymethyl)-6-(2-methoxy-5-((E)-3-oxo-3-(4-(p-tolyl)piperazin-1-yl)-2-(3,4,5-trimethoxyphenyl)prop-1-en-1-yl)phenoxy)tetrahydro-2H-pyran-3,4,5-triyl triacetate ***(32)***. White solid (281 mg, 66%); ^{1}H NMR (600 MHz, DMSO-d_6, *J* in Hz) δ_H 7.03 (s, 1H), 7.02 (s, 1H), 6.97 (s, 1H), 6.94 (d, *J* = 8.4 Hz, 1H), 6.93-6.90 (m, 1H), 6.84 (s, 1H), 6.82 (s, 1H), 6.61 (s, 1H), 6.57 (s, 2H), 5.28 (t, *J* = 9.0 Hz, 1H), 5.03 (d, *J* = 8.4 H, 1Hz), 5.01 (s, 1H), 4.97 (t, *J* = 9.6 Hz, 1H), 4.20 (dd, *J* = 12.0, 5.4 Hz, 1H), 3.95 (dd, *J* = 12.0, 1.8 Hz, 1H), 3.90 (ddd, *J* = 9.6, 5.4, 2.4 Hz, 1H), 3.72 (s, 3H), 3.70 (s, 3H), 3.68 (s, 4H), 3.64 (s, 6H), 3.05 (s, 2H), 3.00 (s, 2H), 2.19 (s, 3H), 2.01 (s, 3H), 2.00 (s, 6H), 1.96 (s, 3H). ^{13}C NMR (150 MHz, DMSO-d_6) δ_C 169.93, 169.53, 169.26, 168.94, 168.80, 153.05, 149.66, 148.68, 145.26, 137.36, 135.21, 130.94, 129.44, 128.57, 128.37, 127.65, 125.05, 119.34, 116.24, 112.61, 105.88, 99.21, 71.83, 70.92, 70.61, 67.86, 61.43, 60.18, 55.92, 55.87, 49.17, 49.00, 46.51, 41.21, 20.47, 20.35, 20.28, 20.04. ESIHRMS *m/z* calcd for $C_{44}H_{52}N_2O_{15}Na^+$ 871.3265 $[M+Na]^+$, found 871.3227.

4.1.4.2.(2S,3R,4R,5S,6R)-2-(acetoxymethyl)-6-(2-methoxy-5-((E)-3-oxo-3-(4-(p-tolyl)piperazin-1-yl)-2-(3,4,5-trimethoxyphenyl)prop-1-en-1-yl)phenoxy)tetrahydro-2H-pyran-3,4,5-triyl triacetate ***(33)***. White solid (287 mg, 68%); ^{1}H NMR (400 MHz,

DMSO-d_6, *J* in Hz) δ_H 7.04 (s, 1H), 7.02 (s, 1H), 6.93 (s, 1H), 6.92 (s, 1H), 6.90 (s, 1H), 6.84 (s, 1H), 6.82 (s, 1H), 6.61 (s, 1H), 6.56 (s, 2H), 5.29 (d, *J* = 1.2 Hz, 1H), 5.17 (s, 1H), 5.16 (s, 1H), 4.92 (d, *J* = 7.2 Hz, 1H), 4.04 (s, 1H), 4.03 (s, 1H), 3.72 (s, 3H), 3.70 (s, 3H), 3.69 (s, 4H), 3.64 (s, 6H), 3.20-3.11 (m, 1H), 3.02 (s, 2H), 3.02 (s, 2H), 2.19 (s, 3H), 2.14 (s, 3H), 2.01 (s, 3H), 1.99 (s, 3H), 1.94 (s, 3H). ^{13}C NMR (100 MHz, DMSO-d_6) δ_C 169.91, 169.70, 169.46, 168.99, 168.75, 153.05, 149.68, 148.66, 145.30, 137.34, 135.27, 130.94, 129.41, 128.60, 128.34, 127.64, 124.96, 119.39, 116.22, 112.65, 105.90, 99.69, 70.22, 70.10, 68.17, 66.95, 60.98, 60.15, 55.93, 55.83, 49.05, 46.32, 41.20, 20.43, 20.35, 20.33, 20.30, 20.01. ESIHRMS *m/z* calcd for $C_{44}H_{52}N_2O_{15}Na^+$ 871.3265 $[M+Na]^+$, found 871.3231.

4.1.4.3.(2R,3S,4S,5R,6S)-2-(acetoxymethyl)-6-(((2S,3S,4R,5S,6R)-4,5-diacetoxy-2-(acetoxymethyl)-6-(2-methoxy-5-((E)-3-oxo-3-(4-(p-tolyl)piperazin-1-yl)-2-(3,4,5-trimethoxyphenyl)prop-1-en-1-yl)phenoxy)tetrahydro-2H-pyran-3-yl)oxy)tetrahydro-2H-pyran-3,4,5-triyl triacetate ***(34)***. White solid (334 mg, 59%); ^{1}H NMR (400 MHz, $CDCl_3$, *J* in Hz) δ_H 7.05 (s, 1H), 7.03 (s, 1H), 6.90 (d, *J* = 2.0 Hz, 1H), 6.86 (dd, *J* = 8.4, 1.6 Hz, 1H), 6.79 (s, 1H), 6.77 (s, 1H), 6.69 (d, *J* = 8.4 Hz, 1H), 6.57 (s, 1H), 6.53 (s, 2H), 5.32 (d, *J* = 2.8 Hz, 1H), 5.16 (t, *J* = 9.2 Hz, 1H), 5.09 (dd, *J* = 7.8, 2.4 Hz, 1H), 5.06 (d, *J* = 1.0 Hz, 1H), 4.92 (dd, *J* = 10.4, 3.2 Hz, 1H), 4.65 (d, *J* = 7.6 Hz, 1H), 4.45 (d, *J* = 8.0 Hz, 1H), 4.29 (dd, *J* = 12.0, 1.8 Hz, 1H), 4.14-4.09 (m, 1H), 4.07 (d, *J* = 4.0 Hz, 1H), 4.05 (dd, *J* = 6.4, 4.8 Hz, 1H), 3.87 (d, *J* = 6.8 Hz, 1H), 3.84 (s, 1H), 3.82-3.62 (m, 4H), 3.80 (s, 3H), 3.74 (s, 3H), 3.68 (s, 6H), 3.49-3.44 (m, 1H), 3.06 (s, 2H), 2.97 (s, 2H), 2.23 (s, 2H), 2.12 (s, 3H), 2.07 (s, 3H), 2.05 (s, 3H), 2.02 (s, 6H), 2.00 (s,

3H), 1.93 (s, 3H). ^{13}C NMR (100 MHz, $CDCl_3$) δ_C 170.35, 170.23, 170.16, 170.13, 170.07, 169.75, 169.50, 169.18, 153.51, 150.34, 148.72, 145.88, 138.09, 135.71, 130.77, 130.30, 129.80, 129.62, 128.02, 125.95, 120.19, 117.05, 112.15, 106.21, 101.18, 100.55, 75.87, 72.67, 72.59, 71.53, 71.12, 70.72, 69.09, 66.75, 61.70, 60.88, 56.18, 56.04, 50.21, 46.93, 41.98, 20.84, 20.80, 20.60, 20.51, 20.49, 20.43. ESIHRMS *m/z* calcd for $C_{56}H_{68}N_2O_{23}Na^+$ 1159.4111 $[M+Na]^+$, found 1159.4074.

*4.1.5. Preparation of Compound **35***

Compound **13** (259 mg, 0.5 mmol) was dissolved in dry DCM with 4 Å molecular sieves, and stirred for 15min at room temperature. Next boron trifluoride diethyl etherate (100 μL, 0.5 mmol) and intermediate **31** (316 mg, 0.6 mmol) were added to the mixture slowly and stirred for 2 h at -40 ℃. After quenching the reaction with triethylamine, the liquid was washed with saturated $NaHCO_3$ solution and brine, dried over Na_2SO_4, and then concentrated. The residue was purified by silica gel chromatography (EtOAc/n-hexane, 1:1) to yield the compound **35**.

*4.1.5.1.(2R,3R,4S,5S,6R)-2-(acetoxymethyl)-6-(2-methoxy-5-((E)-3-oxo-3-(4-(p-tolyl)piperazin-1-yl)-2-(3,4,5-trimethoxyphenyl)prop-1-en-1-yl)phenoxy)tetrahydro-2H-pyran-3,4,5-triyl triacetate **(35)***. White solid (308 mg, 73%); ^{1}H NMR (400 MHz, $CDCl_3$, *J* in Hz) δ_H 7.07 (s, 1H), 7.05 (s, 1H), 6.93 (d, *J* = 1.9 Hz, 1H), 6.87 (dd, *J* = 8.5, 1.8 Hz, 1H), 6.81 (s, 1H), 6.79 (s, 1H), 6.72 (d, *J* = 8.5 Hz, 1H), 6.58 (s, 1H), 6.54 (s, 2H), 5.52 (dd, *J* = 10.0, 3.5 Hz, 1H), 5.44 (dd, *J* = 3.4, 1.8 Hz, 1H), 5.30 (t, *J* = 10.0 Hz, 1H), 5.20 (d, *J* = 1.6 Hz, 1H), 4.23-4.18 (m, 1H), 4.18-4.15 (m, 1H), 4.00 (d, *J* = 10.0 Hz, 1H), 3.84 (s, 3H), 3.79 (s, 3H), 3.69 (s, 6H), 3.05 (s, 2H), 3.03 (s, 2H), 2.25 (s,

3H), 2.17 (s, 3H), 2.04 (s, 3H), 2.02 (s, 3H), 2.00 (s, 3H). ^{13}C NMR (100 MHz, $CDCl_3$) δ_C 170.59, 170.13, 170.02, 169.88, 169.81, 153.64, 150.71, 148.81, 144.62, 138.38, 136.00, 130.82, 130.37, 129.86, 129.49, 128.17, 126.03, 120.31, 117.14, 112.13, 106.22, 97.87, 69.52, 69.45, 68.99, 66.21, 62.30, 60.92, 56.33, 55.95, 50.30, 46.99, 42.00, 20.85, 20.73, 20.48. ESIHRMS *m/z* calcd for $C_{44}H_{52}N_2O_{15}Na^+$ 871.3265 $[M+Na]^+$, found 871.3231.

*4.1.6. General method to synthesize **36-39***

The intermediate **32**-**35** (0.25 mmol) was dissolved in MeOH (10 mL) respectively, and then K_2CO_3 (275 mg, 2 mmol) was added. After stirred for 30 min at room temperature, the residue was purified by silica gel column chromatography to give the desired products **36**-**39**.

*4.1.6.1.(E)-3-(4-methoxy-3-(((2R,3S,4R,5R,6S)-3,4,5-trihydroxy-6-(hydroxymethyl)tetrahydro-2H-pyran-2-yl)oxy)phenyl)-1-(4-(p-tolyl)piperazin-1-yl)-2-(3,4,5-trimethoxyphenyl)prop-2-en-1-one **(36)***. White solid (166 mg, 98%); ^{1}H NMR (400 MHz, DMSO-d_6, *J* in Hz) δ_H 7.04 (s, 1H), 7.02 (s, 1H), 6.93 (s, 1H), 6.89 (d, *J* = 8.4 Hz, 1H), 6.86 (s, 1H), 6.85 (s, 1H), 6.83 (s, 1H), 6.58 (s, 1H), 6.58 (s, 2H), 5.28 (d, *J* = 4.8 Hz, 1H), 5.11 (s, 1H), 5.02 (s, 1H), 4.50 (t, *J* = 5.6 Hz, 1H), 4.42 (d, *J* = 7.6 Hz, 1H), 3.75-3.65 (m, 4H), 3.74 (s, 3H), 3.71 (s, 3H), 3.66 (s, 6H), 3.54 (dd, *J* = 11.2, 4.4 Hz, 1H), 3.45 (dd, *J* = 11.2, 5.6 Hz, 1H), 3.20 (d, *J* = 5.6 Hz, 1H), 3.17 (s, 1H), 3.13 (d, *J* = 8.8 Hz, 1H), 3.04 (s, 4H), 2.93-2.88 (m, 1H), 2.19 (s, 3H). ^{13}C NMR (100 MHz, DMSO-d_6) δ_C 169.03, 153.12, 148.74, 148.70, 145.90, 137.40, 134.41, 131.32, 129.44, 129.04, 128.34, 127.46, 123.59, 116.24, 115.66, 112.03, 106.00, 100.05, 76.80, 76.70,

72.96, 69.17, 60.30, 60.27, 55.95, 55.62, 49.13, 46.49, 41.15, 20.05. ESIHRMS *m/z* calcd for $C_{36}H_{44}N_2O_{11}Na^+$ 703.2843 $[M+Na]^+$, found 703.2812.

4.1.6.2.(E)-3-(4-methoxy-3-(((2R,3S,4R,5S,6S)-3,4,5-trihydroxy-6-(hydroxymethyl)tetrahydro-2H-pyran-2-yl)oxy)phenyl)-1-(4-(p-tolyl)piperazin-1-yl)-2-(3,4,5-trimethoxyphenyl)prop-2-en-1-one ***(37)***. White solid (168 mg, 99%); ^{1}H NMR (400 MHz, DMSO-d_6, *J* in Hz) δ_H 7.04 (s, 1H), 7.02 (s, 1H), 6.90 (s, 1H), 6.87 (s, 1H), 6.85 (s, 1H), 6.85 (s, 1H), 6.83 (s, 1H), 6.59 (s, 1H), 6.57 (s, 2H), 5.10 (d, *J* = 4.4 Hz, 1H), 4.89 (d, *J* = 4.8 Hz, 1H), 4.59 (s, 1H), 4.50 (d, *J* = 3.6 Hz, 1H), 4.38 (d, *J* = 7.6 Hz, 1H), 3.75-3.65 (m, 4H), 3.73 (s, 3H), 3.69 (s, 3H), 3.66 (s, 6H), 3.58-3.53 (m, 1H), 3.53-3.49 (m, 1H), 3.49 (d, *J* = 5.6 Hz, 1H), 3.41 (s, 1H), 3.27-3.23 (m, 1H), 3.20 (t, *J* = 6.4 Hz, 1H), 3.03 (s, 4H), 2.19 (s, 3H). ^{13}C NMR (100 MHz, DMSO-d_6) δ_C 169.01, 153.14, 148.82, 148.71, 146.02, 137.38, 134.55, 131.38, 129.46, 129.10, 128.35, 127.48, 123.41, 116.26, 115.92, 112.06, 106.01, 100.67, 75.18, 73.59, 69.92, 68.08, 60.31, 60.18, 55.93, 55.63, 49.17, 46.50, 41.28, 20.06. ESIHRMS *m/z* calcd for $C_{36}H_{44}N_2O_{11}Na^+$ 703.2843 $[M+Na]^+$, found 703.2808.

4.1.6.3.(E)-3-(3-(((2R,3S,4S,5R,6S)-3,4-dihydroxy-6-(hydroxymethyl)-5-(((2S,3R,4S,5R,6R)-3,4,5-trihydroxy-6-(hydroxymethyl)tetrahydro-2H-pyran-2-yl)oxy)tetrahydro-2H-pyran-2-yl)oxy)-4-methoxyphenyl)-1-(4-(p-tolyl)piperazin-1-yl)-2-(3,4,5-trimethoxyphenyl)prop-2-en-1-one ***(38)***. White solid (206 mg, 98%); ^{1}H NMR (600 MHz, DMSO-d_6, *J* in Hz) δ_H 7.04 (s, 1H), 7.02 (s, 1H), 6.93 (d, *J* = 1.8 Hz, 1H), 6.89 (d, *J* = 9.0 Hz, 1H), 6.85 (s, 1H), 6.84 (d, *J* = 2.4 Hz, 1H), 6.83-6.82 (m, 1H), 6.58 (s, 1H), 6.56 (s, 2H), 5.45 (s, 1H), 5.07 (s, 1H), 4.87 (d, *J* = 7.8 Hz, 1H), 4.81 (s, 1H),

4.69 (s, 1H), 4.60 (s, 1H), 4.58 (s, 1H), 4.53 (d, *J* = 7.8 Hz, 1H), 4.22 (d, *J* = 7.2 Hz, 1H), 3.75-3.65 (m, 4H), 3.73 (s, 3H), 3.69 (s, 3H), 3.65 (s, 6H), 3.62 (d, *J* = 2.7 Hz, 1H), 3.61 (s, 2H), 3.54 (dd, *J* = 10.8, 5.4 Hz, 1H), 3.50 (dd, *J* = 10.8, 7.2 Hz, 1H), 3.47-3.45 (m, 1H), 3.32 (s, 1H), 3.30 (d, *J* = 8.7 Hz, 1H), 3.26 (t, *J* = 8.4 Hz, 1H), 3.15 (dt, *J* = 9.6, 3.6 Hz, 1H), 3.15-2.88 (m, 4H), 2.20 (s, 3H). ^{13}C NMR (150 MHz, DMSO-d_6) δ_C 168.97, 153.10, 148.74, 148.69, 145.77, 137.35, 134.48, 131.31, 129.44, 129.03, 128.32, 127.44, 123.50, 116.24, 115.91, 112.02, 105.93, 103.85, 99.69, 79.77, 75.56, 75.19, 74.83, 73.36, 72.71, 70.61, 68.16, 60.44, 60.28, 59.88, 55.96, 55.59, 48.98, 46.61, 41.22, 20.06. ESIHRMS *m/z* calcd for $C_{42}H_{54}N_2O_{16}Na^+$ 865.3371 $[M+Na]^+$, found 865.3380.

4.1.6.4.(E)-3-(4-methoxy-3-(((2R,3S,4S,5S,6R)-3,4,5-trihydroxy-6-(hydroxymethyl)tetrahydro-2H-pyran-2-yl)oxy)phenyl)-1-(4-(p-tolyl)piperazin-1-yl)-2-(3,4,5-trimethoxyphenyl)prop-2-en-1-one ***(39)***. White solid (165 mg, 97%); ^{1}H NMR (400 MHz, DMSO-d_6, *J* in Hz) δ_H 7.07 (d, *J* = 2.0 Hz, 1H), 7.04 (s, 1H), 7.01 (s, 1H), 6.88 (d, *J* = 8.8 Hz, 1H), 6.84 (s, 1H), 6.82 (s, 1H), 6.80 (d, *J* = 1.6 Hz, 1H), 6.60 (s, 1H), 6.56 (s, 2H), 5.10 (d, *J* = 1.6 Hz, 1H), 4.96 (d, *J* = 2.0 Hz, 1H), 4.86 (s, 1H), 4.80 (s, 1H), 4.36 (t, *J* = 5.2 Hz, 1H), 3.80 (s, 1H), 3.75-3.65 (m, 4H), 3.73 (s, 3H), 3.68 (s, 3H), 3.65 (s, 6H), 3.59-3.53 (m, 1H), 3.52 (d, *J* = 11.6 Hz, 1H), 3.48 (s, 1H), 3.46 (d, *J* = 3.6 Hz, 1H), 3.44 (d, *J* = 3.2 Hz, 1H), 3.03 (s, 4H), 2.19 (s, 3H). ^{13}C NMR (100 MHz, DMSO-d_6) δ_C 168.96, 153.07, 150.09, 148.71, 144.97, 137.50, 134.77, 131.09, 129.44, 128.91, 128.34, 127.74, 123.96, 119.99, 116.26, 112.25, 105.96, 100.18, 74.94, 70.68,

70.12, 66.59, 60.97, 60.23, 55.94, 55.78, 49.10, 46.57, 41.31, 20.05. ESIHRMS *m/z* calcd for $C_{36}H_{44}N_2O_{11}Na^+$ 703.2843 $[M+Na]^+$, found 703.2809.

4.2. Measurement of octanol-water partition coefficient (log P)

Compound **13** (4mg), each kind of sugar conjugate (4mg) and CA-4 (4mg) were dissolved in 1 mL of n-octanol (saturated with water) in a 10 mL Vial, the solution was placed for 24 h at room temperature. After centrifugation at 10,000 rpm/min for 10 min, the supernatant was taken out and mixed with equal volume of water (saturated with n-octanol). Next, the mixture was allowed to stand at room temperature for 24 h, centrifuged at 10,000 rpm/min for 20 min, and then separated organic and aqueous phases carefully. The concentrations of the compounds in the organic and aqueous phase were measured by standard concentration curves equation which were established by liquid chromatography. $\log P = \log (C_{n\text{-octanol}}/C_{water})$ was calculated by corresponding concentration of compounds in the n-octanol and water phase.

4.3. Cell lines and materials for biological studies

Cell counting kit-8 were purchased from Dojindo company (Dojindo Laboratories, Kumamoto, Japan). 96-well plates, 24-well plates and 6-well plates were purchased from Corning incorporated. HCT116 (human colon cancer cells), A549 (human non-small cell lung cancer cells), AGS (human gastric adenocarcinoma cells), SK-MES-1 (human lung squamous cell carcinoma cells) cell strains were purchased from Cell Bank of Chinese Academy of Sciences (Shanghai, China). NCM460 (human normal colonic epithelial cells) was purchased from Cellverse Bioscience Technology Co., Ltd. Ham’s F-12K (Kaighn’s) Medium (F-12K), dulbecco's modifified Eagle's medium

(DMEM), McCoy's 5A (Modified) and Fetal bovine serum (FBS) were purchased from Gibco company, Roswell Park Memorial Institute 1640 medium (RPMI-1640) was purchased from Cellverse Bioscience Technology Co., Ltd..

4.4. Cytotoxicity assay

Cells were seeded into 96-well plates (2×10^3 cells/well). HCT116 were cultured overnight in McCoy's 5A (16600082) containing 10% FBS, A549 and AGS were maintained overnight in F-12K (21127022) containing 10% FBS, SK-MES-1 were cultured overnight in DEME (10566016) supplemented with 10% FBS, NCM460 were maintained overnight in RPMI-1640 (iCell-0002) with 10% FBS. Different concentrations of compounds and negative control (0.1% DMSO) were added respectively then incubated at 37 ℃ for 72 h. Cell viability was assayed by Cell Counting Kit-8. After co-incubation with 10% CCK8 for 2 h, the absorbance of the cells was measured at 450 nm. Cell survival rate of the compounds were calculated as (As-Ab)/(Ac-Ab) × 100% (As: absorbance of sample wells; Ab: absorbance of blank wells; Ac: absorbance of control wells). IC_{50} value corresponding to the concentration that caused 50% inhibition of cell proliferation was calculated by GraphPad Prism.

4.5. Cell Invasion

Matrigel (356234, BD, USA) was diluted with pre-chilled serum-free medium at a volume ratio of 1 : 3, and then coated uniformly in a pre-cooled Transwell (3422, Corning, USA) and exposed to ultraviolet radiation at 37 ℃ for 2 h. After digestion, the HCT116 cells were resuspended in serum-free medium and were inoculated into the upper chamber of the transwell (1×10^4 cells/well). After adding complete medium to

stimulate cell invasion, the cells were treated with different concentrations of **13** in a 5% CO_2 incubator at 37 ℃ for 48 h, with control group DMSO (0.1%). The cells were fixed by 4% paraformaldehyde (P1110, Solarbio, China) for 20 min. After washing by PBS, the transwell was dried on the cover of the culture plate in order, and 0.1% crystal violet dye was added to the outer membrane of the transwell for 20 min. Fluorescent inverted microscope (Boshida, BD-YGD-2) and Image J were used to analysis cell invasion.

4.6. Cell migration

The procedure of cell migration assay is similar to cell invasion assay despite the matrigel was not coated on the transwell. The HCT116 cells were inoculated into the upper chamber of the transwell (1×10^4 cells/well). After adding complete medium to stimulate cell migration, the cells were treated with different doses of **13** at 37 ℃ for 24 h in a 5% CO_2 incubator, with negative control DMSO (0.1%). Likewise, the cells were fixed by 4% paraformaldehyde (P1110, Solarbio, China) for 20min and then washed by PBS. Next, the transwell was dried on the culture plate in order, 0.1% crystal violet dye was used to stain for 20 min. Cell migration was analyzed by fluorescent inverted microscope (Boshida, BD-YGD-2) and Image J.

4.7. Immunofluorescent staining assay of tubulin

HCT116 cells were processed into a suspension (1×10^5 cells/well) after digesting with Trypsin-EDTA (0.25%) (SH30042.01, Hyclone, USA) and re-suspending in complete culture medium. And 200 uL were taken out, then placed on the glass slides (WHB-24-CS, WHB, China). The cells were incubated in a 5% CO_2 incubator at 37 ℃ overnight. And then cells were treated with different concentrations of compound **13** or

DMSO (0.1%) for 48 h in a 5% CO_2 incubator at 37 ℃. The cells were washed with PBS, and fixed by 4% paraformaldehyde (P1110, Solarbio, China) for 15 min. Next, the cells were washed with PBS and then permeabilized in 0.5% Triton X-100 (93443, Sigma, USA) for 20 min. Subsequently, the cells were blocked in Immunol Staining Blocking Buffer (P0102, Beyotime, China) at 37 ℃ for 30 min. And then the cells were incubated with Monoclonal Anti-α-Tubulin Clone B-5-1-2 (1:4000, Cat. No. T5168, Sigma-Aldrich, USA) at 4 ℃ overnight. Following washes in PBST (P1031, Solarbio, China) for 3 times, cells were incubated with Anti-mouse IgG (H+L), $F(ab')_2$ Fragment (Alexa Fluor® 488 Conjugate) (1:1000, #CST4408, Cell Signaling Technology, USA) in dark for 1 h at room temperature. Finally, after adding the Antifade Mounting Medium with DAPI (P0131, Beyotime, China) to the glass slides, fluorescent inverted microscope (Boshida, BD-YGD-2) and confocal microscope (Carl Zeiss LSM710) were used to study the HCT116 cytoskeleton.

4.8. Cell cycle assay

Analyses of the cell cycle were performed by using flow cytometry. HCT116 cells and A549 cells were seed in 6-well plates (2.5×10^5 cells/well), and incubated in a 5% CO_2 incubator at 37 ℃ for 24 h and then treated with different concentrations of compound **13** for 24 h, with control group DMSO (0.1%). Cells were centrifuged at 1,000 rpm for 5min, and washed with ice-cold PBS. Then the cells were fixed in 70% EtOH (pre-chilled) at 4 ℃ overnight. Cell were stained with 0.5 mL of PI/RNase Staining Buffer (BD, Cat. No. 550825, USA) in dark for 15 min at room temperature.

Finally, the cells were determined by flow cytometry using Novocyte D2060R (Agilent, USA), and analyzed by FlowJo V10.

4.9. Cell apoptosis analysis

Analyses of the cell apoptosis were performed by using flow cytometry. A549 cells were seed in 6-well plates (2.5×10^5 cells/well), and incubated in a 5% CO_2 incubator at 37 ℃ for 24 h and then treated with different concentrations of compound **13** or DMSO (0.1%) for 24 h. The cells were collected and washed by PBS and then treated with 500 μL of 1 x Annexin V Binding Buffer. After incubating with 5 μL Annexin V-APC Reagent and 5 μL PI Reagent (Elabscience Biotechnology Co.,Ltd., Cata. E-CK-A217, China) for 20 min in the dark at room temperature, Novocyte D2060R (Agilent, USA) was used to determine the cell apoptosis.

4.10. Western blot analysis

HCT-116 cells were treated with compound **13** at different doses for 24 h or 48 h. And then the cells were washed with PBS (pre-chilled) and lysed with lysis buffer (P0013B, Beyotime, China) on ice for 10 min. Subsequently, the cells were centrifuged at 14,000 rpm for 5 min. Collected the supernatants and the protein concentration was detected with BCA protein assay kit (BL521, Biosharp, China). The extracts were reconstituted within loading buffer and inactivated for 10 min at 100 ℃. And then the proteins were fractionated by 10%-12.5% sodium dodecyl sulfate polyacrylamide gel electrophoresis (SDS-PAGE), and transferred to polyvinylidene difluoride (PVDF) (IPVH00010, MILLIPORE, USA). The proteins were blocked with 5% skimmed milk and incubated with appropriate dilution of primary antibodies, including β-Actin

(1:1000, #CST4970, Cell Signaling Technology, USA), Cyclin B1 (1:1000, #CST12231, Cell Signaling Technology, USA), Cdc2 (1:1000, #CST28439, Cell Signaling Technology, USA), LC3A/B (1:1000, #CST12741, Cell Signaling Technology, USA) and Phospho-SQSTM1/p62 (1:1000, #CST16177, Cell Signaling Technology, USA) at 4 °C overnight. These above primary antibodies were washed and then incubated with Anti-rabbit IgG, HRP-linked Antibody (1:1000, #CST7074, Cell Signaling Technology, USA) for 1 h. A chemiluminescence reagent (WLA006, Wanleibio, China) was used to enhance the immunoreactive protein bands.

4.11. Immunofluorescent staining assay of autophagy

HCT116 cells were seed on the glass slides in 6-well plates, and incubated in a 5% CO_2 incubator at 37 ℃ for overnight. 5 μL of mRFP-GFP-LC3 (HBAD-1007, Hanbio, China) adenovirus were added into each well when the cell confluence rate reached 50%. The cells were incubated in a 5% CO_2 incubator at 37 ℃ for 24 h and then were treated with different concentrations of compound **13** or DMSO (0.1%) for 24 h. The cells were fixed by 4% paraformaldehyde (P1110, Solarbio, China) for 15 min and washed with PBS for 2-3 times. Subsequently, the cells were blocked in Antifade Mounting Medium with DAPI (P0131, Beyotime, China). Fluorescent inverted microscope (Boshida, BD-YGD-2) and confocal microscope (Carl Zeiss LSM710) were used to analysis the autophagy of HCT116 cells.

4.12. Tumor nude mice model

Xenografts of HCT116 cells were established by subcutaneous injection into 5 weeks old female BALB/c nude mice (inspection certificate number:

NO.110011221106805175, Beijing Vital River Laboratory Animal Technology Co., Ltd, China). The cells (5×10^7/0.2 mL/mouse) were inoculated on the side of the right forelimb. Tumor growth was observed regularly, when the tumor volume reached 100 mm^3, mice were divided at random into four groups by mice weight and tumor size. The solvent control group were injected of normal saline (intraperitoneal injection). Cisplatin (5mg/kg) group were intraperitoneally injected every 3 days, compound **13** (20 mg/kg and 40 mg/kg) groups were treated every 2 days by intraperitoneal injection. Body weights and tumor volumes were monitored during treatment of 20 days. Finally, mice were euthanized and tumors were weighed. The tumor size were measured by vernier caliper and he tumor volume was calculated according to the formula of $W^2 \times L/2$ (W = tumor's short diameter, L = tumor's long diameter). The tumor growth inhibition (TGI) were calculated according to the following formula: TGI (%) = (1-V1/V2) × 100% (V1 = average tumor volume in the treatment group; V2 = average tumor volumes in the control group).

4.13. Molecular Docking analysis

The molecular docking simulations were conducted by using Molecular Operating Environment (MOE, Chemical Computing Group Inc., Montreal, Canada) v 2018. 01. The 3D structure of protein tubulin was downloaded from RCSB Protein Data Bank with PDB ID of 5LYJ. The 2D structures of the small molecules were drawn in ChemBioDraw 2014 and were converted to 3D conformations through energy minimization. The protein structure was prepared by using the Structure Preparation module in MOE. Prior to dock, the force field of AMBER10: EHT and the implicit

solvation model of Reaction Field (R-field) were selected. The “induced fit” protocol was selected, in which the side chains of the binding site in receptor were allowed to move according to ligand conformations, and a constraint was applied on their positions. The weight used for tethering side chain atoms to their original positions was 10. The binding mode was visualized by PyMOL.

Declaration of competing interest

The authors declare that they have no known competing financial interests or personal relationships that could have appeared to influence the work reported in this paper.

Acknowledgments

This project was supported by the National Natural Science Foundation of China (Nos. 22177023), the Key Science and Technology Program of Hainan Province (No. ZDKJ202008), the Hainan Provincial Natural Science Foundation of China (221RC1054).

References

[1] R.L. Siegel, K.D. Miller, A. Jemal, Cancer statistics, 2015, CA Cancer J Clin, 65 (2015) 5-29. https://doi.org/10.3322/caac.21254

[2] R. Li, Y. Wu, Y. Li, W. Shuai, A. Wang, Y. Zhu, X. Hu, Y. Xia, L. Ouyang, G. Wang, Targeted regulated cell death with small molecule compounds in colorectal cancer: Current perspectives of targeted therapy and molecular mechanisms, Eur J Med Chem, 265 (2024) 116040. https://doi.org/10.1016/j.ejmech.2023.116040

[3] Y. Yang, P. Liu, M. Zhou, L. Yin, M. Wang, T. Liu, X. Jiang, H. Gao, Small-molecule drugs of colorectal cancer: Current status and future directions, Biochim Biophys Acta Mol Basis Dis, 1870 (2024) 166880. https://doi.org/10.1016/j.bbadis.2023.166880

[4] E. Dekker, P.J. Tanis, J.L.A. Vleugels, P.M. Kasi, M.B. Wallace, Colorectal cancer, Lancet, 394 (2019) 1467-1480. https://doi.org/10.1016/S0140-6736(19)32319-0

[5] R.L. Siegel, K.D. Miller, N.S. Wagle, A. Jemal, Cancer statistics, 2023, CA Cancer J Clin, 73 (2023) 17-48. https://doi.org/10.3322/caac.21763

[6] S. Vodenkova, T. Buchler, K. Cervena, V. Veskrnova, P. Vodicka, V. Vymetalkova, 5-fluorouracil and other fluoropyrimidines in colorectal cancer: Past, present and future, Pharmacol Ther, 206 (2020) 107447. https://doi.org/10.1016/j.pharmthera.2019.107447
[7] J. Souglakos, N. Ziras, S. Kakolyris, I. Boukovinas, N. Kentepozidis, P. Makrantonakis, S. Xynogalos, C. Christophyllakis, C. Kouroussis, L. Vamvakas, V. Georgoulias, A. Polyzos, Randomised phase-II trial of CAPIRI (capecitabine, irinotecan) plus bevacizumab vs FOLFIRI (folinic acid, 5-fluorouracil, irinotecan) plus bevacizumab as first-line treatment of patients with unresectable/metastatic colorectal cancer (mCRC), Br J Cancer, 106 (2012) 453-459. https://doi.org/10.1038/bjc.2011.594
[8] R. Siegel, C. DeSantis, K. Virgo, K. Stein, A. Mariotto, T. Smith, D. Cooper, T. Gansler, C. Lerro, S. Fedewa, C. Lin, C. Leach, R.S. Cannady, H. Cho, S. Scoppa, M. Hachey, R. Kirch, A. Jemal, E. Ward, Cancer treatment and survivorship statistics, 2012, CA Cancer J Clin, 62 (2012) 220-241. https://doi.org/10.3322/caac.21149
[9] G.R. Pettit, S.B. Singh, M.R. Boyd, E. Hamel, R.K. Pettit, J.M. Schmidt, F. Hogan, Antineoplastic Agents. 291. Isolation and Synthesis of Combretastatins A-4, A-5, and A-6, Journal of Medicinal Chemistry, 38 (1995) 1666-1672. https://doi.org/10.1021/jm00010a011
[10] C. Zhang, Y. Qu, X. Ma, M. Li, S. Li, Y. Li, L. Wu, NQO1-selective activated prodrugs of combretastatin A-4: Synthesis and biological evaluation, Bioorg Chem, 103 (2020) 104200. https://doi.org/10.1016/j.bioorg.2020.104200
[11] A. Faouzi, A. Arnaud, A. Bancet, C. Barette, J. Preto, C.V. Do, L.P. Jordheim, Z. Bousfiha, T.T.B. Nguyen, M. Verriere, A. Farce, M.O. Fauvarque, R. Barret, T. Lomberget, Combretastatin A-4 sulfur-containing heterocyclic derivatives: Synthesis, antiproliferative activities and molecular docking studies, Eur J Med Chem, 215 (2021) 113275. https://doi.org/10.1016/j.ejmech.2021.113275
[12] M. Ashraf, T.B. Shaik, M.S. Malik, R. Syed, P.L. Mallipeddi, M. Vardhan, A. Kamal, Design and synthesis of cis-restricted benzimidazole and benzothiazole mimics of combretastatin A-4 as antimitotic agents with apoptosis inducing ability, Bioorg Med Chem Lett, 26 (2016) 4527-4535. https://doi.org/10.1016/j.bmcl.2016.06.044
[13] G.R. Pettit, M.R. Rhodes, D.L. Herald, E. Hamel, J.M. Schmidt, R.K. Pettit, Antineoplastic Agents. 445. Synthesis and Evaluation of Structural Modifications of (Z)- and (E)-Combretastatin A-4, Journal of Medicinal Chemistry, 48 (2005) 4087-4099. https://doi.org/10.1021/jm0205797
[14] R. Romagnoli, P.G. Baraldi, M.K. Salvador, D. Preti, M. Aghazadeh Tabrizi, A. Brancale, X.H. Fu, J. Li, S.Z. Zhang, E. Hamel, R. Bortolozzi, G. Basso, G. Viola, Synthesis and evaluation of 1,5-disubstituted tetrazoles as rigid analogues of combretastatin A-4 with potent antiproliferative and antitumor activity, J Med Chem, 55 (2012) 475-488. https://doi.org/10.1021/jm2013979
[15] X.E. Jian, F. Yang, C.S. Jiang, W.W. You, P.L. Zhao, Synthesis and biological evaluation of novel pyrazolo[3,4-b]pyridines as cis-restricted combretastatin A-4 analogues, Bioorg Med Chem Lett, 30 (2020) 127025. https://doi.org/10.1016/j.bmcl.2020.127025
[16] N.G. Barnes, A.W. Parker, A.A. Ahmed Mal Ullah, P.A. Ragazzon, J.A. Hadfield, A 2-step synthesis of Combretastatin A-4 and derivatives as potent tubulin assembly inhibitors, Bioorg Med Chem, 28 (2020) 115684. https://doi.org/10.1016/j.bmc.2020.115684
[17] J.A. Hadfield, K. Gaukroger, N. Hirst, A.P. Weston, N.J. Lawrence, A.T. McGown, Synthesis and evaluation of double bond substituted combretastatins, Eur J Med Chem, 40 (2005) 529-541. https://doi.org/10.1016/j.ejmech.2004.12.008

[18] C. Borrel, S. Thoret, X. Cachet, D. Guenard, F. Tillequin, M. Koch, S. Michel, New antitubulin derivatives in the combretastatin A4 series: synthesis and biological evaluation, Bioorg Med Chem, 13 (2005) 3853-3864. https://doi.org/10.1016/j.bmc.2005.02.039
[19] H. Chen, Y. Li, C. Sheng, Z. Lv, G. Dong, T. Wang, J. Liu, M. Zhang, L. Li, T. Zhang, D. Geng, C. Niu, K. Li, Design and synthesis of cyclopropylamide analogues of combretastatin-A4 as novel microtubule-stabilizing agents, J Med Chem, 56 (2013) 685-699. https://doi.org/10.1021/jm301864s
[20] P. Zhou, Y. Liu, L. Zhou, K. Zhu, K. Feng, H. Zhang, Y. Liang, H. Jiang, C. Luo, M. Liu, Y. Wang, Potent Antitumor Activities and Structure Basis of the Chiral beta-Lactam Bridged Analogue of Combretastatin A-4 Binding to Tubulin, J Med Chem, 59 (2016) 10329-10334. https://doi.org/10.1021/acs.jmedchem.6b01268
[21] D. Simoni, G. Grisolia, G. Giannini, M. Roberti, R. Rondanin, L. Piccagli, R. Baruchello, M. Rossi, R. Romagnoli, F.P. Invidiata, S. Grimaudo, M.K. Jung, E. Hamel, N. Gebbia, L. Crosta, V. Abbadessa, A. Di Cristina, L. Dusonchet, M. Meli, M. Tolomeo, Heterocyclic and Phenyl Double-Bond-Locked Combretastatin Analogues Possessing Potent Apoptosis-Inducing Activity in HL60 and in MDR Cell Lines, Journal of Medicinal Chemistry, 48 (2005) 723-736. https://doi.org/10.1021/jm049622b
[22] Q. Zhang, Y. Peng, X.I. Wang, S.M. Keenan, S. Arora, W.J. Welsh, Highly Potent Triazole-Based Tubulin Polymerization Inhibitors, Journal of Medicinal Chemistry, 50 (2007) 749-754. https://doi.org/10.1021/jm061142s
[23] T.M. Beale, P.J. Bond, J.D. Brenton, D.S. Charnock-Jones, S.V. Ley, R.M. Myers, Increased endothelial cell selectivity of triazole-bridged dihalogenated A-ring analogues of combretastatin A-1, Bioorg Med Chem, 20 (2012) 1749-1759. https://doi.org/10.1016/j.bmc.2012.01.010
[24] Y.H. Li, B. Zhang, H.K. Yang, Q. Li, P.C. Diao, W.W. You, P.L. Zhao, Design, synthesis, and biological evaluation of novel alkylsulfanyl-1,2,4-triazoles as cis-restricted combretastatin A-4 analogues, Eur J Med Chem, 125 (2017) 1098-1106. https://doi.org/10.1016/j.ejmech.2016.10.051
[25] M. Mustafa, D. Abdelhamid, E.M.N. Abdelhafez, M.A.A. Ibrahim, A.M. Gamal-Eldeen, O.M. Aly, Synthesis, antiproliferative, anti-tubulin activity, and docking study of new 1,2,4-triazoles as potential combretastatin analogues, Eur J Med Chem, 141 (2017) 293-305. https://doi.org/10.1016/j.ejmech.2017.09.063
[26] R. Schobert, B. Biersack, A. Dietrich, K. Effenberger, S. Knauer, T. Mueller, 4-(3-Halo/amino-4,5-dimethoxyphenyl)-5-aryloxazoles and -N-methylimidazoles that are cytotoxic against combretastatin A resistant tumor cells and vascular disrupting in a cisplatin resistant germ cell tumor model, J Med Chem, 53 (2010) 6595-6602. https://doi.org/10.1021/jm100345r
[27] A. Kamal, D. Dastagiri, M.J. Ramaiah, E.V. Bharathi, J.S. Reddy, G. Balakishan, P. Sarma, S.N. Pushpavalli, M. Pal-Bhadra, A. Juvekar, S. Sen, S. Zingde, Synthesis, anticancer activity and mitochondrial mediated apoptosis inducing ability of 2,5-diaryloxadiazole-pyrrolobenzodiazepine conjugates, Bioorg Med Chem, 18 (2010) 6666-6677. https://doi.org/10.1016/j.bmc.2010.07.067
[28] V.R. Patel, W.S. Park, An Evolving Role of Piperazine Moieties in Drug Design and Discovery, Mini-Reviews in Medicinal Chemistry, 13 (2013) 1579-1601. https://doi.org/http://dx.doi.org/10.2174/13895575113139990073
[29] M. Asif, Piperazine and Pyrazine containing molecules and their diverse pharmacological activities, International Journal of Advances in Scientific Research, 1 (2015) 05. https://doi.org/10.7439/ijasr.v1i1.1766

[30] M. Gerlach, E. Claus, S. Baasner, G. Muller, E. Polymeropoulos, P. Schmidt, E. Gunther, J. Engel, Design and synthesis of a focused library of novel aryl- and heteroaryl-ketopiperazides, Arch Pharm (Weinheim), 337 (2004) 695-703. https://doi.org/10.1002/ardp.200400623
[31] M.E. Welsch, S.A. Snyder, B.R. Stockwell, Privileged scaffolds for library design and drug discovery, Curr Opin Chem Biol, 14 (2010) 347-361. https://doi.org/10.1016/j.cbpa.2010.02.018
[32] H. Prinz, A.K. Ridder, K. Vogel, K.J. Bohm, I. Ivanov, J.B. Ghasemi, E. Aghaee, K. Muller, N-Heterocyclic (4-Phenylpiperazin-1-yl)methanones Derived from Phenoxazine and Phenothiazine as Highly Potent Inhibitors of Tubulin Polymerization, J Med Chem, 60 (2017) 749-766. https://doi.org/10.1021/acs.jmedchem.6b01591
[33] Y. Yin, F. Qiao, L.Y. Jiang, S.F. Wang, S. Sha, X. Wu, P.C. Lv, H.L. Zhu, Design, synthesis and biological evaluation of (E)-3-(3,4-dihydroxyphenyl)acrylylpiperazine derivatives as a new class of tubulin polymerization inhibitors, Bioorg Med Chem, 22 (2014) 4285-4292. https://doi.org/10.1016/j.bmc.2014.05.029
[34] K. Ohsumi, R. Nakagawa, Y. Fukuda, T. Hatanaka, Y. Morinaga, Y. Nihei, K. Ohishi, Y. Suga, Y. Akiyama, T. Tsuji, Novel Combretastatin Analogues Effective against Murine Solid Tumors: Design and Structure−Activity Relationships, Journal of Medicinal Chemistry, 41 (1998) 3022-3032. https://doi.org/10.1021/jm980101w
[35] X. Qi, S. Jiang, Z. Hui, Y. Gao, Y. Ye, F. Lirussi, C. Garrido, L. Xu, X. He, R. Bai, X.Y. Ye, T. Xie, Design, synthesis and antitumor efficacy evaluation of a series of novel beta-elemene-based macrocycles, Bioorg Med Chem, 74 (2022) 117049. https://doi.org/10.1016/j.bmc.2022.117049
[36] X. Zhang, F. Hu, L. Liu, B. Xu, Effect of silencing of mediator of DNA damage checkpoint protein 1 on the growth of oral squamous cell carcinoma in vitro and in vivo, Eur J Oral Sci, 127 (2019) 494-499. https://doi.org/10.1111/eos.12662
[37] Y. Yu, Q. Peng, P. Zhao, L. Wang, Y. Weng, X. Chen, X. Li, S. Feng, X. Wang, W. Lu, X. Xie, X. Cheng, Inhibition of invasion and metastasis in choriocarcinoma by migration and invasion inhibitory protein, Placenta, 130 (2022) 46-52. https://doi.org/10.1016/j.placenta.2022.10.015
[38] Y. Tan, H. Hu, W. Zhu, T. Wang, T. Gao, H. Wang, J. Chen, J. Xu, S. Xu, H. Zhu, Design, synthesis and biological evaluation of novel dihydroquinolin-4(1H)-one derivatives as novel tubulin polymerization inhibitors, Eur J Med Chem, 262 (2023) 115881. https://doi.org/10.1016/j.ejmech.2023.115881
[39] K. Mahal, B. Biersack, S. Schruefer, M. Resch, R. Ficner, R. Schobert, T. Mueller, Combretastatin A-4 derived 5-(1-methyl-4-phenyl-imidazol-5-yl)indoles with superior cytotoxic and anti-vascular effects on chemoresistant cancer cells and tumors, Eur J Med Chem, 118 (2016) 9-20. https://doi.org/10.1016/j.ejmech.2016.04.045
[40] Q.K. Shen, H. Deng, S.B. Wang, Y.S. Tian, Z.S. Quan, Synthesis, and evaluation of in vitro and in vivo anticancer activity of 14-substituted oridonin analogs: A novel and potent cell cycle arrest and apoptosis inducer through the p53-MDM2 pathway, Eur J Med Chem, 173 (2019) 15-31. https://doi.org/10.1016/j.ejmech.2019.04.005
[41] C.J. Wang, X. Guo, R.Q. Zhai, C. Sun, G. Xiao, J. Chen, M.Y. Wei, C.L. Shao, Y. Gu, Discovery of penipanoid C-inspired 2-(3,4,5-trimethoxybenzoyl)quinazolin-4(3H)-one derivatives as potential anticancer agents by inhibiting cell proliferation and inducing apoptosis in hepatocellular carcinoma cells, Eur J Med Chem, 224 (2021) 113671. https://doi.org/10.1016/j.ejmech.2021.113671

[42] J. Yan, Y. Pang, J. Sheng, Y. Wang, J. Chen, J. Hu, L. Huang, X. Li, A novel synthetic compound exerts effective anti-tumour activity in vivo via the inhibition of tubulin polymerisation in A549 cells, Biochem Pharmacol, 97 (2015) 51-61. https://doi.org/10.1016/j.bcp.2015.07.008
[43] L.A. Roser, P. Erkoc, R. Ingelfinger, M. Henke, T. Ulshofer, A.K. Schneider, V. Laux, G. Geisslinger, I. Schmitt, R. Furst, S. Schiffmann, Lecanoric acid mediates anti-proliferative effects by an M phase arrest in colon cancer cells, Biomed Pharmacother, 148 (2022) 112734. https://doi.org/10.1016/j.biopha.2022.112734
[44] Y. Zhang, J. Tang, C. Wang, Q. Zhang, A. Zeng, L. Song, Autophagy-related lncRNAs in tumor progression and drug resistance: A double-edged sword, Genes Dis, 11 (2024) 367-381. https://doi.org/10.1016/j.gendis.2023.04.015
[45] J. Ao, F. Zeng, L. Wang, L. Qiu, R. Cao, X. Li, Design, synthesis and pharmacological evaluation of beta-carboline derivatives as potential antitumor agent via targeting autophagy, Eur J Med Chem, 246 (2023) 114955. https://doi.org/10.1016/j.ejmech.2022.114955
[46] X. Lu, C. Zhu, C. Zhang, X. Li, Z. Yu, Z. Zhang, X. Shi, Design, synthesis and biological evaluation of 3-aryl-7-hydroxy scopoletin derivatives as autophagy activators against tumorigenesis, Eur J Med Chem, 244 (2022) 114805. https://doi.org/10.1016/j.ejmech.2022.114805
[47] T. Kaizuka, H. Morishita, Y. Hama, S. Tsukamoto, T. Matsui, Y. Toyota, A. Kodama, T. Ishihara, T. Mizushima, N. Mizushima, An Autophagic Flux Probe that Releases an Internal Control, Mol Cell, 64 (2016) 835-849. https://doi.org/10.1016/j.molcel.2016.09.037
[48] K. Singh, A. Sharma, M.C. Mir, J.A. Drazba, W.D. Heston, C. Magi-Galluzzi, D. Hansel, B.P. Rubin, E.A. Klein, A. Almasan, Autophagic flux determines cell death and survival in response to Apo2L/TRAIL (dulanermin), Molecular Cancer, 13 (2014) 70. https://doi.org/10.1186/1476-4598-13-70
[49] Y. Peng, X. Li, P. Gu, W. Cheng, R. Zhang, K. Hu, Curcumin-loaded zein/pectin nanoparticles: Caco-2 cellular uptake and the effects on cell cycle arrest and apoptosis of human hepatoma cells (HepG2), Journal of Drug Delivery Science and Technology, 74 (2022). https://doi.org/10.1016/j.jddst.2022.103497
[50] R. Gaspari, A.E. Prota, K. Bargsten, A. Cavalli, M.O. Steinmetz, Structural Basis of cis- and trans-Combretastatin Binding to Tubulin, Chem, 2 (2017) 102-113. https://doi.org/10.1016/j.chempr.2016.12.005